(12) INTERNATIONAL APPLICATION PUBLISHED UNDER THE PATENT COOPERATION TREATY (PCT)

(19) World Intellectual Property Organization
International Bureau

(43) International Publication Date
09 November 2017 (09.11.2017)

WIPO | PCT

(10) International Publication Number
WO 2017/191265 A1

(51) International Patent Classification:
H01L 51/42 (2006.01) *H01L 27/30* (2006.01)

(21) International Application Number:
PCT/EP2017/060675

(22) International Filing Date:
04 May 2017 (04.05.2017)

(25) Filing Language: English

(26) Publication Language: English

(30) Priority Data:
16168403.0 04 May 2016 (04.05.2016) EP
16172226.9 31 May 2016 (31.05.2016) EP

(71) Applicant: **NOVALED GMBH** [DE/DE]; Tatzberg 49, 01307 Dresden (DE).

(72) Inventors: **RINCON, Maria Cristina Momblona**; C/Alboraya 32, 46010 Valencia (ES). **ESCRIG, Lidon Gil**; C/Llucena n 7, 12132 Atzeneta del Maestrat, Castellon (ES). **SESSOLO, Michele**; Calle Azagador de Alboaya 16-7, 46020 Valencia (ES). **BOLINK, Jan Hendrik**; Calle Xaloc 29-35, 46116 Moncada (ES). **BLOCHWITZ-NIMOTH, Jan**; Tannenstraße 6c, 01097 Dresden (DE). **LEDERER, Kay**; Boltenhagener Str. 3, 01109 Dresden (DE).

(74) Agent: **BOEHMERT & BOEHMERT**; BITTNER, Thomas L., Hollerallee 32, 28209 Bremen (DE).

(81) Designated States *(unless otherwise indicated, for every kind of national protection available)*: AE, AG, AL, AM, AO, AT, AU, AZ, BA, BB, BG, BH, BN, BR, BW, BY, BZ, CA, CH, CL, CN, CO, CR, CU, CZ, DE, DJ, DK, DM, DO, DZ, EC, EE, EG, ES, FI, GB, GD, GE, GH, GM, GT, HN, HR, HU, ID, IL, IN, IR, IS, JP, KE, KG, KH, KN, KP, KR, KW, KZ, LA, LC, LK, LR, LS, LU, LY, MA, MD, ME, MG, MK, MN, MW, MX, MY, MZ, NA, NG, NI, NO, NZ, OM, PA, PE, PG, PH, PL, PT, QA, RO, RS, RU, RW, SA, SC,

(54) Title: SOLAR CELL

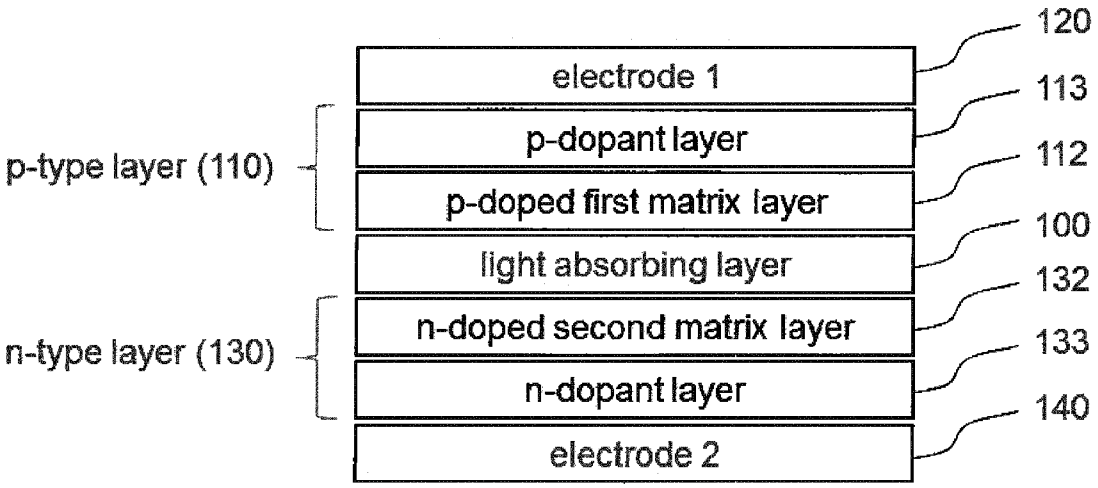

Fig. 3

(57) Abstract: The present disclosure refers to a solar cell, having a first electrode, a second electrode, and a stack of layers provided between the first and second electrode. The stack of layers comprises a light absorbing layer comprising an absorber compound provided with a perovskite crystal structure, an organic ρ-type layer provided between the first electrode and the light absorbing layer, and a n-type layer provided between the second electrode and the first light absorbing layer. The organic ρ-type layer comprises at least one of a layer comprising an organic ρ-type dopant, and a layer comprising a mixture of an organic ρ-type dopant and a first organic aromatic matrix compound. The n-type layer comprises at least one of a layer comprising an n-type dopant, and a layer comprising of a mixture of an n-type dopant and a second organic aromatic matrix compound.

WO 2017/191265 A1

[Continued on next page]

SD, SE, SG, SK, SL, SM, ST, SV, SY, TH, TJ, TM, TN, TR, TT, TZ, UA, UG, US, UZ, VC, VN, ZA, ZM, ZW.

(84) Designated States *(unless otherwise indicated, for every kind of regional protection available)*: ARIPO (BW, GH, GM, KE, LR, LS, MW, MZ, NA, RW, SD, SL, ST, SZ, TZ, UG, ZM, ZW), Eurasian (AM, AZ, BY, KG, KZ, RU, TJ, TM), European (AL, AT, BE, BG, CH, CY, CZ, DE, DK, EE, ES, FI, FR, GB, GR, HR, HU, IE, IS, IT, LT, LU, LV, MC, MK, MT, NL, NO, PL, PT, RO, RS, SE, SI, SK, SM, TR), OAPI (BF, BJ, CF, CG, CI, CM, GA, GN, GQ, GW, KM, ML, MR, NE, SN, TD, TG).

Published:

— *with international search report (Art. 21(3))*

Solar cell

The present disclosure relates to a solar cell.

Background

Thin-film photovoltaic is a key technology among future low cost and sustainable renewable energy sources. Organic-inorganic (hybrid) lead halide perovskite solar cells have been proposed for photovoltaic applications because of their impressive power conversion efficiencies (PCEs), now exceeding 21%. (see Kojima et al., J. Am. Chem. Soc. 131, 6050-6051 (2009); Lee et al., Science 338, 643-647 (2012); Yang et al., Science 348, 1234-1237 (2015)).The perovskite thin-film absorber can be deposited by simple solution or sublimation methods, hence with a large potential for the preparation of inexpensive photovoltaic devices. The high PCEs are the result of the very high absorption coefficient and mobilities of the photogenerated electrons and holes of hybrid perovskites.

In order to prepare high performance solar cells, homogeneous perovskite films with a high degree of crystallinity are needed in order to reduce the trap concentration and achieve an adequate mobility of the charge carriers (see Nie et al., Science 347, 522-525 (2015)). While the use of the archetype perovskite, methylammonium lead iodide ($MAPbI_3$), can lead to high efficiency devices, a further decrease of the bandgap by incorporation of formamidinium (FA), allows for the harvesting of additional near-infrared photons (see Pellet et al., Angewandte Chemie International Edition 53, 3151-3157 (2014)).When such a mixed organic cation perovskite is further stabilized by replacing part of the iodide with bromide, the champion material for perovskite cells, $(FAPbI_3)_{1-x}(MAPbBr_3)_x$, is obtained (see Yang et al., Science 348, 1234-1237 (2015); Jeon et al., Nature 517, 476-480 (2015); Bi et al., Science Advances 2 (2016)).

Different solar cell architectures have been used. One of them derives from dye-sensitized solar cells, and consists of a transparent conductive substrate coated with a mesoporous or planar TiO_2 layer (n-type, hence acting as the electron transport layer, ETL) into or onto which the perovskite light absorbing layer is applied. A hole transport layer (HTL, p-type), usually consisting of organic semiconductors is then deposited from solution on top of the perovskite and the device is finished with an evaporated top electrode (see Stranks et al., Science 342, 341-344 (2013); Eperon et al., Advanced Functional Materials 24, 151-157 (2014); Conings et al., Advanced Materials 26, 2041-2046 (2014); and Chen et al., Journal of the American Chemical Society 136, 622-625 (2014)).

Another configuration is inverted compared to the above mentioned one, and the conductive substrate is coated with a HTL, followed by the perovskite absorber and an ETL, coated with a suitable evaporated top electrode (see Wu et al., Energy & Environmental Science 8, 2725-2733 (2015); Zhou et al., Science 345, 542-546 (2014). While these two device configuration have been identified as "conventional" and "inverted", such devices may rather be referred to as n-i-p device and p-i-n device. A detailed explanation of n-i-p and p-i-n devices will be provided in the summary.

Chen et al. (Science 350, 944-948 (2015)) demonstrated that the PCE in planar devices may be limited by the conductivity of the metal oxide layers, which can be increased by doping these layers. This was achieved by incorporating heteroatoms with different valences into the solution processed metal oxides, although leading only to a small increase in the conductivity (approximately one order of magnitude). Thus, only very thin metal oxide transport layers (<20 nm) could be used otherwise PCE would drop significantly. We propose a more versatile strategy to control the conductivity of charge transport layers in perovskite devices is the use of doped organic semiconductors. These materials are used in organic light-emitting diodes and also in small molecular weight organic solar cells.

In doped organic semiconductors the conductivity can be varied over several orders of magnitude by increasing the doping concentration. However, it is unknown as of yet, if the incorporation of such doped layers would yield enough charge carrier transport for perovskite solar cells without conflicting with other key PV parameters such as PCE, FF, Voc and lifetime, hence degrading overall performance. Contrary to an OLED (organic light emitting diodes) no external voltage is applied, and contrary to the case in organic photovoltaic devices (which typically use thinner absorption layers and several absorber units connected in series) the current density is larger.

Most reported organic-inorganic (hybrid) lead halide perovskite solar cells that are employing a vacuum deposited perovskite light absorbing layer do then employ charge transport layers processed from solution. Fully vacuum processed solar cell devices would offer the additional advantage of being compatible with temperature sensitive substrates, allowing for conformal coatings on non-planar substrates and for the straightforward implementation into tandem solar cells (see Polander et al., APL Materials 2, 081503 (2014)). Besides the high sophistication level of the deposition systems required for vacuum processing, they have

been implemented in the electronic industry since long demonstrating high throughput and reliability (Ono et al., Journal of Materials Chemistry A (2016)).

By selecting certain hole transport molecules with regard to the energy levels of the conduction and valence band of the perovskite, open circuit voltages (Voc) as high as 1.1 V were demonstrated (Polander et al., APL Materials 2, 081503 (2014); Kim et al., Organic Electronics 17, 102-106 (2015), Ono et al., Journal of Materials Chemistry A (2016)). The highest efficiency (15.4%) was measured for a device with rather high hysteresis (14.0 % PCE was obtained for the same cell measured in the opposite bias scan direction), which used single layers of undoped organic molecules as the charge extraction layers (see Ke et al., Journal of Materials Chemistry A 3, 23888-23894 (2015)). This is in line with the conclusions of Berhe et al., Energy Environ. Sci., 2016, 9, 323-356 that high stability and lifetime of perovskite solar cells can rather be achieved with solution processed perovskite absorbers.

Electrically doped perovskite layers and their use as light absorbing and / or charge transport layers in optoelectronic devices is disclosed in document EP 2 942 826 A2.

Document WO 2012 / 175219 A1 relates to an electronic device. A solar cell may comprise a sequence of two layers: C_{60} / C_{60} : compound between an active layer (SubPc) and an electrode (Al). Compound is a molecular n-type dopant comprising an organic compound (i.e. N1,N4-bis(tri-p-tolylphosphoranylidene)benzene-1,4-diamine (PhIm)).

State of the art solar cells may suffer from low open-circuit voltage, low short-circuit current, low efficiency, short lifetime and / or low fill factor.

Summary

It is an object of the present disclosure to provide a solar cell which overcomes drawbacks of the prior art. In particular, it is an object to provide a solar cell having improved open-circuit voltage, short-circuit current, efficiency, lifetime and/ or high fill factor.

A solar cell according to claim 1 is provided. Alternative embodiments are disclosed in the dependent claims.

A solar cell comprises a first electrode and a second electrode and at least one stack of layers provided between the first electrode and the second electrode. The at least one stack of layers comprises a first light absorbing layer provided with a layer thickness of about 200 nm to about 700 nm, and comprises an absorber compound provided with a perovskite crystal structure.

In one aspect, a solar cell is provided, comprising:

- a first electrode;
- a second electrode; and
- at least one stack of layers provided between the first electrode and the second electrode, the at least one stack of layers comprising
  - a first light absorbing layer provided with a layer thickness of about 200 nm to about 700 nm, and comprising an absorber compound provided with a perovskite crystal structure;
  - a first organic p-type layer provided between the first electrode and the first light absorbing layer, the first organic p-type layer comprising at least one of
    - a layer comprising an organic p-type dopant; and
    - a layer comprising a mixture of an organic p-type dopant and a first organic aromatic matrix compound;

  wherein, for the first organic p-type layer, the following is provided:
  - the first organic aromatic matrix compound has a molecular weight of about 400 to about 1500;
  - the organic p-type dopant has a molecular weight of about 350 to about 1700;
  - the first oxidation potential of the first organic aromatic matrix compound is equal to or less negative compared to N2,N2,N2',N2',N7,N7,N7',N7'-octakis(4-methoxyphenyl)-9,9'-spirobi[fluorene]-2,2',7,7'-tetraamine and equal or less positive than 1,3-bis(carbazol-9-yl)benzene when measured under the same conditions by cyclic voltammetry against Fc/Fc^+ in dichloromethane solution; and
  - the first reduction potential of the organic p-type dopant is equal to or more positive compared to 2,3,5,6-Tetrafluor-7,7,8,8-tetracyanochinodimethan when measured by cyclic voltammetry against Fc/Fc^+ in acetonitrile; and
  - a first n-type layer provided between the second electrode and the first light absorbing layer, the first n-type layer comprising at least one of
    - a layer comprising an n-type dopant; and
    - a layer comprising a mixture of an n-type dopant and a second organic aromatic matrix compound;

wherein, for the first n-type layer, the following is provided:

- the second organic aromatic matrix compound has a molecular weight of about 300 to about 1500; and
- the first reduction potential of the second organic aromatic matrix compound is in the range of about ± 1.0 V, preferably ± 0.5 V, compared to the reduction potential of C_{60} when measured under the same conditions by cyclic voltammetry against Fc/Fc^+ in acetonitrile; and
- the n-type dopant is one of
  - a molecular dopant comprising an organic compound having a molecular weight of about 300 to about 1500, and
  - a metal dopant selected from the group consisting of a metal halide having a molecular weight of about 25 to about 500, a metal complex having a molecular weight of about 150 to about 1500, and a zero-valent metal selected from the group consisting of alkali metal, alkaline earth metal, and rare earth metals.

The first organic p-type layer may consist of at least one of a layer consisting of an organic p-type dopant; and a layer consisting of a mixture of an organic p-type dopant and a first organic aromatic matrix compound.

The first n-type layer may consist of at least one of a layer consisting of an n-type dopant; and a layer consisting of a mixture of an n-type dopant and a second organic aromatic matrix compound.

In an embodiment the first organic p-type layer is in direct contact with the first electrode and with the first light absorbing layer. Thereby, good performance is achieved.

The first organic aromatic matrix compound has a molecular weight of about 400 to about 1500. The organic p-type dopant has a molecular weight of about 350 to about 1700.

In an embodiment the first organic aromatic matrix compound has a molecular weight of about 500 to about 1300.

In another embodiment the organic p-type dopant has a molecular weight of about 350 to about 800.

If the molecular weight is in this rage, suitable evaporation rate may be achieved during vacuum thermal deposition.

The first oxidation potential of the first organic aromatic matrix compound is equal to or less negative compared to N2,N2,N2',N2',N7,N7,N7',N7'-octakis(4-methoxyphenyl)-9,9'-spirobi[fluorene]-2,2',7,7'-tetraamine, which is about -0.07 V, and equal or less positive than 1,3-bis(carbazol-9-yl)benzene, which is about 0.93 V, when measured under the same conditions by cyclic voltametry against Fc/Fc+ in dichloromethane solution at room temperature.

In an embodiment the first oxidation potential of the first organic aromatic matrix compound is more positive than about -0.07 V and less positive than about 0.70 V when measured under the same conditions by cyclic voltametry against Fc/Fc+ in dichloromethane solution at room temperature.

In another embodiment the first oxidation potential of the first organic aromatic matrix compound is more positive than about -0.07 V and less positive than about 0.50 V when measured under the same conditions by cyclic voltametry against Fc/Fc+ in dichloromethane solution at room temperature.

The first reduction potential of the organic p-type dopant is equal to or more positive compared to 2,3,5,6-Tetrafluor-7,7,8,8-tetracyanochinodimethan, which is about 0.18 V, when measured by cyclic voltametry against Fc/Fc+ in acetonitrile at room temperature.

In an embodiment the first reduction potential of the organic p-type dopant is equal or more positive than of 2,2'-(perfluoronaphthalene-2,6-diylidene) dimalononitrile, which is about 0.25 V, when measured under the same conditions by cyclic voltametry against Fc/Fc+ in acetonitrile solution at room temperature. High conductivity of the doped layer may be achieved, when the p-type dopant is selected in this range.

A first n-type layer is provided between the second electrode and the first light absorbing layer.

In an embodiment the first organic n-type layer is in direct contact with the second electrode and with the first light absorbing layer.

The second organic aromatic matrix compound has a molecular weight of about 300 to about 1500.

In another embodiment the second organic aromatic matrix compound has a molecular weight of about 400 to about 800.

The first reduction potential of the second organic aromatic matrix compound is in the range of about ± 1.00 V compared to the reduction potential of C60, which is about -1.00 V, when measured under the same conditions by cyclic voltametry against Fc/Fc+ in acetonitrile at room temperature.

In an embodiment the first reduction potential of the second organic aromatic matrix compound is more negative than -0.50 V and less negative than -1.50 V when measured under the same conditions by cyclic voltametry against Fc/Fc+ in acetonitrile at room temperature.

In another embodiment the first reduction potential of the second organic aromatic matrix compound is about -1.00 V when measured under the same conditions by cyclic voltametry against Fc/Fc+ in acetonitrile at room temperature.

The n-type dopant is either a molecular dopant comprising an organic compound having a molecular weight of about 300 to about 1500, or a metal compound selected from the group consisting of a metal halide having a molecular weight of about 25 to about 500, a metal complex having a molecular weight of about 150 to about 1500, and a zero-valent metal selected from the group consisting of alkali, alkaline earth, and rare earth metals.

In an embodiment the n-type dopant is an organic molecular dopant having a molecular weight of about 300 to about 1200.

In another embodiment the n-type dopant is a molecular dopant and the first oxidation potential is more negative than about -0.20 V and less negative than about -1.00 V , when measured under the same conditions by cyclic voltametry against Fc/Fc+ in dichloromethane solution at room temperature.

In a further embodiment the n-type dopant is a molecular dopant and the first oxidation potential is more negative than about -0.40 V and less negative than about -0.70 V , when

measured under the same conditions by cyclic voltametry against Fc/Fc+ in dichloromethane solution at room temperature.

In a further embodiment the n-type dopant is a metal compound selected from the group of metal halide having a molecular weight of about 25 to about 250.

In a further embodiment the n-type dopant is a metal complex having a molecular weight of about 150 to about 1000.

In another embodiment the n-type dopant may be one of an alkali halide, and a metal complex selected from the group of alkali metal organic complex and main group and transition metal paddle-wheel complexes.

In a further embodiment the n-type dopant is a zero-valent metal selected from the group of Li, Na, K, Rb, Cs, Mg, Ca, Sr, Ba, Eu, Yb and Sm.

In another embodiment the n-type dopant is a zero-valent metal selected from the group of Li, Mg, Eu, Yb and Sm.

The light absorbing layer according to the disclosure comprises at least one absorber compound. The absorber compound may have a stoichiometry of AMX_3 or A_2MX_4, where "A" and "M" are cations and "X" is an anion. The "A" and "M" cations can have a variety of charges and in the original Perovskite mineral ($CaTiO_3$), the A cation is divalent and the M cation is tetravalent. The term "perovskite" as used here refers to the "perovskite crystal structure", but not limited to the specific structure of the perovskite material, $CaTiO_3$. "Perovskite" may encompass any material that has the same type of crystal structure as calcium titanium oxide, and materials in which the bivalent cation is replaced by two separate monovalent cations. The perovskite formulae as used here may include structures having three or four anions, which may be the same or different, and/or one or two organic cations, and / or metal atoms carrying two or three positive charges. Organic-inorganic perovskites are hybrid materials exhibiting combined properties of organic composites and inorganic crystallinity. The inorganic component forms a framework bound by covalent and ionic interactions, which provide high carrier mobility. The organic component helps in the self-assembly process of those materials. It also enables the hybrid materials to be deposited by low-cost technique as other organic materials. Additional important property of the organic component is to tailor the electronic properties of the organic-inorganic material by reducing

its dimensionality and the electronic coupling between the inorganic sheets.

In another embodiment, A is a monovalent or bivalent cation. In another embodiment, A is selected from the group of monovalent or bivalent ammonium cations and alkali metal cations and alkaline earth metal cations.

In a further embodiment A is independently selected from organic, monovalent cations selected from primary, secondary, tertiary or quaternary organic ammonium compounds, including N-containing heteroaryl rings and ring systems, A having from 1 to 60 carbons and 1 to 20 heteroatoms; or being an organic, bivalent cation selected from primary, secondary, tertiary or quaternary organic ammonium compounds having from 1 to 60 carbons and 2 to 20 heteroatoms and having two positively charged nitrogen atoms; or being selected from the group of alkaline metals and/or alkaline earth metals.

In another embodiment A is the methyl ammonium (MA) cation $[(CH_3)_3N]^+$ or alkali metal cation or a combination thereof.

In an embodiment, M is a divalent metal cation or a trivalent metal cation. In another embodiment, M is a divalent metal cation selected from the group consisting of Cu^{2+}, Ni^{2+}, Co^{2+}, Fe^{2+}, Mn^{2+}, Cr^{2+}, Pd^{2+}, Cd^{2+}, Ge^{2+}, Sn^{2+}, Pb^{2+}, Eu^{2+}, or Yb^{2+} or a trivalent metal cation selected from the group consisting of Bi^{3+} and Sb^{3+}. In still a further embodiment, M is selected from the group consisting of Pd^{2+}, Sn^{2+}.

In an embodiment X is a monovalent anion. In another embodiment X is independently selected from Cl^-, Br^-, I^-, NCS^-, CN^-, and NCO^-. In a further embodiment, X is selected from I^-, Cl^-, and Br^-.The at least one stack of layers may further comprise at least one of a first undoped organic performance enhancement layer arranged between the organic p-type layer and the first light absorbing layer; and a second undoped organic performance enhancement layer arranged between the organic n-type layer and the first light absorbing layer. The undoped organic performance enhancement layer may comprise at least one of the first and the second organic matrix compound. The undoped organic performance enhancement layer does neither contain an organic p-type dopant nor an n-type dopant.

In another embodiment the first undoped organic performance enhancement layer is in direct contact with the first organic p-type layer and with the first light absorbing layer.

In an embodiment the first undoped organic performance enhancement layer comprises the first organic aromatic matrix compound.

In another embodiment the second undoped organic performance enhancement layer is in direct contact with the second organic p-type layer and with the first light absorbing layer.

In a further embodiment the second undoped organic performance enhancement layer comprises the second organic aromatic matrix compound.

The solar cell may further comprise at least one of a second n-type layer provided between the first electrode and the at least one stack of layers; and a second organic p-type layer provided between the at least one stack of layers and the second electrode. The second n-type layer may be equal to or different from the first n-type layer. The second organic p-type layer may be equal to or different from the first organic p-type layer. With regard to different layer design, one or more of the parameters provided for the layers may be different for the first and second layer.

In an embodiment the second n-type layer is in direct contact with the first electrode and with the at least one stack of layers.

In another embodiment the second organic p-type layer is in direct contact with the second electrode and with the at least one stack of layers.

The solar cell may further comprise a second light absorbing layer arranged between the first stack of layers and one of the first and the second electrode.

In an embodiment the second light absorbing layer is a solar cell.

In another embodiment the second light absorbing layer comprises a light absorbing layer selected from the group of silicon (Si), copper-indium-gallium-diselenide (CIDS), cadmium-telluride (CdTe) and an organic light absorbing layer.

In a further embodiment the second light absorbing layer is in direct contact with the first stack of layers and one of the first or the second electrode.

The solar cell may comprise at least two stacks of layers arranged between the first and the second electrode. The at least two stacks of layers may be provided in direct contact.

In an embodiment at least one undoped interlayer may be arranged between neighboring stacks of layers.

The first organic aromatic matrix compound may be selected from the group consisting of triarylamine, carbazole, thiophene, phthalocyanine, diphenylhydrazone, and quinoxaline. The second organic aromatic matrix compound may be selected from the group consisting of acridine, benzoacridine, dibenzoacridine, anthracene, pyrene, triazine, and xanthene.

In an embodiment the first oxidation potential of the n-type dopant may be equal or less positive than (1,3-dicyclohexyl-4,5-dimethyl-1H-imidazol-3-ium-2-yl)triphenylborate, which is 0.89 V, when measured under the same conditions by cyclic voltametry against Fc/Fc^+ in dichloromethane solution at room temperature.

The organic p-type dopant may be provided with a concentration of about 3 wt% to about 50 wt% in the organic p-type layer.

In an embodiment the organic p-type dopant may be provided with a concentration of about 5 wt% to about 15 wt%.

The n-type dopant in the n-type layer may be provided with a concentration, in case of a molecular dopant, of about 3 wt% to about 60 wt%. In case of a metal dopant, in the n-type layer, the n-type dopant may be provided with a concentration about 0.5 mol% to about 10 mol%.

In an embodiment the molecular n-type dopant in the n-type layer may be provided with a concentration of about 15 wt% to about 45 wt%.

In the at least one stack of layers, at least one of the following may be provided: the organic p-type layer is having a layer thickness of about 25 nm to about 1000 nm. In an embodiment the organic p-type layer is having a thickness of about 30 to about 500nm. In another embodiment the organic p-type layer is having a thickness of about 30 to about 150 nm.

The n-type layer is having a layer thickness of about 25 nm to about 1000 nm. In an embodiment the n-type layer is having a thickness of about 30 nm to about 500 nm. In another embodiment the n-type layer is having a thickness of about 30 to about 150 nm.

In a further embodiment the undoped organic performance enhancement layer is having a thickness of about 5 nm to about 30 nm.

A method to determine the ionization potentials (IP) is the ultraviolet photo spectroscopy (UPS). It is usual to measure the ionization potential for solid state materials; however, it is also possible to measure the IP in the gas phase. Both values are differentiated by their solid state effects, which are, for example the polarization energy of the holes that are created during the photo ionization process. A typical value for the polarization energy is approximately 1 eV, but larger discrepancies of the values can also occur. The IP is related to onset of the photoemission spectra in the region of the large kinetic energy of the photoelectrons, i.e. the energy of the most weakly bounded electrons. A related method to UPS, the inverted photo electron spectroscopy (IPES) can be used to determine the electron affinity (EA). However, this method is less common. Electrochemical measurements in solution are an alternative to the determination of solid state oxidation (E_{ox}) and reduction (E_{red}) potential. An adequate method is, for example, cyclic voltametry. To avoid confusion, the claimed energy levels are defined in terms of comparison with reference compounds having well defined redox potentials in cyclic voltametry, when measured by a standardized procedure. A simple rule is very often used for the conversion of redox potentials into electron affinities and ionization potential: IP (in eV) = 4.8 eV + e^*E_{ox} (wherein E_{ox} is given in volts vs. ferrocenium/ferrocene (Fc^+/Fc)) and EA (in eV) = 4.8 eV + e^*E_{red} (E_{red} is given in volts vs. Fc^+/Fc) respectively (see B.W. D'Andrade, Org. Electron. 6, 11-20 (2005)), e* is the elemental charge. Conversion factors for recalculation of the electrochemical potentials in the case other reference electrodes or other reference redox pairs are known (see A.J. Bard, L.R. Faulkner, „Electrochemical Methods: Fundamentals and Applications", Wiley, 2. Ausgabe 2000). The information about the influence of the solution used can be found in N.G. Connelly et al., Chem. Rev. 96, 877 (1996). It is usual, even if not exactly correct, to use the terms „energy of the HOMO" $E_{(HOMO)}$ and "energy of the LUMO" $E_{(LUMO)}$, respectively, as synonyms for the ionization energy and electron affinity (Koopmans Theorem). It has to be taken into consideration that the ionization potentials and the electron affinities are usually reported in such a way that a larger value represents a stronger binding of a released or of an absorbed electron, respectively. The energy scale of the frontier molecular orbitals (HOMO, LUMO) is opposed to this. Therefore, in a rough approximation, the following

equations are valid: IP = $-E_{(HOMO)}$ and EA = $E_{(LUMO)}$ (the zero energy is assigned to the vacuum).

For certain materials, such as hole transport materials, the ionization potential of the material may be >5.30eV.

In the context of the present disclosure, the term "doped" refers to a dopant which increases electrical conductivity of the doped layer. The p-type dopant and n-type dopant of the present disclosure are essentially non-emissive dopants. The term "essentially non-emissive" means that the contribution of the non-light-emitting dopant to the emission spectrum from the device is less than 10 %, preferably less than 5 % relative to the emission spectrum.

In another aspect, the term "doped" may refer to electrical doping. An effect of "electrical doping" is an increase of the conductivity through the presence of the dopant in the layer.

The solar cell may be a p-i-n device or a n-i-p device. The terms "p-i-n" and "n-i-p" describe the layer sequence in the at least one stack of layers. In p-i-n device the deposition of the layer sequence of the at least one stack of layers begins with the p-type layer 110 followed by the light absorbing layer 100 followed by the n-type layer 130. In n-i-p device the deposition of layer sequence of the at least one stack of layers begins with the n-type layer 130 followed by the light absorbing layer 100 followed by the n-type layer 110. A common expert term for light absorbing layer is also "intrinsic layer". The term "p-i-n" arises from the sequence p-type layer/intrinsic layer/n-type layer. The term "n-i-p" arises from the sequence n-type layer/intrinsic layer/p-type layer.

In an embodiment the first electrode of the p-i-n solar cell device is transparent and illumination of the solar cell is done through the first electrode and the p-type layer. In another embodiment the second electrode of the n-i-n solar cell device is transparent and illumination of the solar cell is done through the second electrode and the n-type layer.

In a further embodiment the transparent electrode material is a thin conductive oxide (TCO).

In another embodiment the transparent electrode material is selected from the group of indium-tin-oxide (ITO), aluminum-zinc-oxide (AZO), indium-gallium-zinc-oxide (IGZO), indium-zink-oxide (IZO), molybdenum-zink-oxide (MZO) and indium-molybdenum-oxide (IMO).

In another embodiment the transparent electrode material is selected from the group of magnesium (Mg), aluminum (Al), aluminum-lithium (Al-Li), calcium (Ca), magnesium-indium (Mg-In), magnesium-silver (Mg-Ag), silver (Ag), gold (Au), or the like.

In an embodiment the first electrode is the cathode and the second electrode is the anode.

In the present specification the following terms are defined shall be applied unless a different definition is given in the claims or elsewhere in this specification.

In the context of the present specification the term "room temperature" refers to a temperature of about 20 to about 25 °C, preferably of about 22 °C.

Cyclic Voltametry (CV) is an electrochemical technique which measures the current that develops in an electrochemical cell under conditions where voltage is in excess of that voltage predicted by the Nernst equation for a given compound. CV is performed by cycling the potential of a working electrode, and measuring the resulting current.

Cyclic voltametry is used to determine the first oxidation potential and the first reduction potential.

The first oxidation potential is the potential at which the investigated compound looses one electron.

The first reduction potential is the potential at which the investigated compound gains one electron.

In an embodiment the first organic matrix compound is TaTm (N4,N4,N4",N4"-tetra([1,1'-biphenyl]-4-yl)-[1,1':4',1"-terphenyl]-4,4"-diamine) and the first oxidation potential is 0.40 V when measured under the same conditions by cyclic voltametry against Fc/Fc+ in dichloromethane solution at room temperature.

In an embodiment the first organic matrix compound is TaDi (N3,N3'-di([1,1'-biphenyl]-4-yl)-N3,N3'-dimesityl-[1,1'-biphenyl]-3,3'-diamine) and the first oxidation potential is 0.49 V when measured under the same conditions by cyclic voltametry against Fc/Fc+ in dichloromethane solution at room temperature.

In an embodiment the second organic matrix compound is C_{60} and the first reduction potential is about -1.00 V when measured under the same conditions by cyclic voltametry against Fc/Fc+ in acetonitrile solution at room temperature.

In an embodiment the organic p-type dopant is F6-TCNNQ and the first reduction potential is about 0.25 V when measured under the same conditions by cyclic voltametry against Fc/Fc+ in acetonitrile solution at room temperature.

In another embodiment the organic p-type dopant is CyTa (2,2',2''-(cyclopropane-1,2,3-triylidene)tris(2-(p-cyanotetrafluorophenyl)acetonitrile)) and the first reduction potential is about 0.25 V when measured under the same conditions by cyclic voltametry against Fc/Fc+ in acetonitrile solution at room temperature.

In an embodiment the n-type dopant is the organic n-type dopant PhIm (N1,N4-bis(tri-p-tolylphosphoranylidene)benzene-1,4-diamine) and the first oxidation potential is about -0.46 V when measured under the same conditions by cyclic voltametry against Fc/Fc+ in dichloromethane solution at room temperature.

In an embodiment the light absorbing layer comprises an absorber compound of the formula $CH_3NH_3PbI_3$. This absorber compound is having a first oxidation potential comparable to the oxidation potential of TaTm when measured under the same conditions by cyclic voltametry against Fc/Fc+ in dichloromethane solution at room temperature.

As used herein, „wt%" stands for weight percentage and refers to a composition of matrix compound and dopant. It specifies the concentration of the dopant as a fraction of the total weight of the composition of matrix compound and dopant.

As used herein, „mol%" stands for molar percentage and refers to a composition of matrix compound and dopant. It specifies the number of moles of the dopant as a fraction of the total number of moles in the composition of matrix compound and dopant.

All numeric values are herein assumed to be prefixed by the term "about", whether or not explicitly indicated. As used herein, the term "about" refers to variation in the numerical quantity that can occur. Whether or not modified by the term „about" the claims include equivalents to the quantities.

It should be noted that, as used in this specification and the appended claims, the singular forms „a", „an", and „the" include plural referents unless the content clearly dictates otherwise.

The term "does not contain" does not include impurities. Impurities have no technical effect with respect to the object achieved by the present disclosure.

The term "molecular weight" is a physical property defined as the mass of a given substance (chemical element or chemical compound) divided by the molar amount of substance (number of mols). The base SI unit for molecular weight is kg/mol. For historical reasons, molecular weights are almost always expressed in g/mol. The molecular weight may be calculated from standard atomic masses. It is the sum of all standard atomic masses in a compound. The standard atomic masses are given in the periodic table of elements. Experimentally, the molecular weight may be determined by mass spectrometry, from the vapour density, freezing-point depression or boiling point elevation.

In the context that the undoped organic performance enhancement layers and do not contain a dopant specifies that no dopant has been added deliberately to the layer composition.

According to another aspect of the present disclosure, there is provided a method of manufacturing a solar cell, the method using deposition via vacuum thermal evaporation.

It was surprisingly found that the solar cell according to at least one aspect of the present disclosure solves the problem underlying the present disclosure by being superior over the solar cells known in the art, in particular with respect to initial performance and lifetime. The inventors have surprisingly found that particular good performance can be achieved when using, for example, a p-type layer between the first electrode and the first light absorbing layer and using an n-type layer between the second electrode and the first light absorbing layer.

Description of embodiments

Following, further aspects are disclosed by referring to Figures. In the figures show:

Fig. 1 a schematic representation of a solar cell in p-i-n (Fig. 1a) and n-i-p (Fig. 1b) layer sequence;

Fig. 2 a schematic representation of a reference solar cell;

Fig. 3 a schematic representation of a solar cell provided with a p-doped first matrix layer and n-doped second matrix layer;

Fig. 4 a schematic representation of a solar cell provided with a p-doped layer and an n-dopant layer;

Fig. 5 a schematic representation of a solar cell provided with a p-doped p-matrix layer and an n-doped n-matrix layer;

Fig. 6 a schematic representation of a solar cell provided with undoped organic performance enhancement layers;

Fig. 7 a schematic representation of a solar cell provided with an n-type layer and a p-type layer on both sides of a light absorbing layer;

Fig. 8 a schematic representation of a solar cell provided with a second light absorbing layer;

Fig. 9 a schematic representation of a solar cell provided with a first and a second stack of layers;

Fig. 10 a schematic representation of a solar cell provided with more than two stacks of layers;

Fig. 11 a schematic representation of a solar cell with a plurality of stacks of layers wherein between neighbouring stacks of layers an interlayer is provided;

Fig. 12 a graphical representation of the current density (J) vs. voltage for the best-performing p-i-n and n-i-p solar cells;

Fig. 13 a graphical representation of the effect of leaving out the performance enhancement layer on lifetime of the solar cell represented as open circuit voltage (V_{OC}) vs operating time (Time);

Fig. 14 a graphical representation of the effect of variation in organic p-type dopant concentration on lifetime of the solar cell represented as power conversion efficiency (PCE) vs operating time (Time); and

Fig. 15 a graphical representation of the effect of variation in n-type dopant concentration on on lifetime of the solar cell represented as power conversion efficiency (PCE) vs operating time (Time)

Following, alternative embodiments for a solar cell are described with reference to Fig. 1 to 12. Fig. 2 shows a schematic representation of a reference solar cell.

Referring to Fig. 1, 3 to 11, the solar cell is provided with a first and a second electrode 120, 140. Between the first and the second electrode 120, 140 a light absorbing layer 100 is

provided. The light absorbing layer comprises an absorber compound provided with a perovskite crystal structure. The absorber compound may have a stoichiometry of AMX_3, where "A" and "M" are cations and "X" is an anion. By the first and second electrode 120, 140 an anode and a cathode are implemented, thereby, a n-i-p device and a p-i-n device may be provided.

The reference solar cell shown in Fig. 2 is provided with a first and a second electrode 200, 210, and a light absorbing layer 220 sandwiched between the first and the second electrode 200, 210. By the electrodes 200, 210 an anode and a cathode are implemented. Between the light absorbing layer 220 and the first and second electrode 200, 210 electrically undoped charge transport layers 230, 240 are arranged.

Fig. 1 shows a schematic representation of a solar cell wherein between the first and the second electrode 120, 140, in addition to the light absorbing layer 100, a p-type layer 110 and an n-type layer 130 are provided. The light absorbing layer 100, the p-type layer 110, and the n-type layer 130 are provided in a stack of layers 150 which, for the embodiment shown in Fig. 1, is in direct contact with the first and the second electrode 120, 140. In p-i-n device the deposition of the layer sequence of the solar cell begins with the first electrode 120. In n-i-p device the deposition of layer sequence of the solar cell begins with the second electrode 140.

Fig. 3 shows a schematic representation of a solar cell wherein between the first and the second electrode 120, 140, in addition to the light absorbing layer 100, both the p-type layer 110 and the n-type layer 130 are provided with a two layers structure. The p-type layer 110 comprises a p-doped first matrix layer 112 and a p-dopant layer 113. The n-type layer 130 comprises an n-doped second matrix layer 132 and an n-dopant layer 133.

Fig. 4 shows a schematic representation of a solar cell which, compared to the solar cell in Fig. 3, is missing both the p-doped first matrix layer 112 and the n-doped second matrix layer 132. Fig. 5 shows a schematic representation of a solar cell which, compared to the solar cell in Fig. 3, is missing the p-dopant layer 113 and the n-dopant layer 133.

Fig. 6 shows a schematic representation of a solar cell which, compared to the solar cell in Fig. 1, comprises a first and a second electrically undoped organic performance enhancement layer 111, 131 provided on both sides of the light absorbing layer 100.

Fig. 7 shows a schematic representation of a solar cell which on both sides of the light absorbing layer 100 is provided with a combination of a p-type layer 110a, 110b and an n-type layer 130a, 130b. With regard to layer design parameters, the n-type layers 130a, 130b may be equal to each or different from each other. Similarly, the p-type layers 110a, 110b maybe equal to or different from each other regarding one or more layer design parameters.

Fig. 8 shows a schematic representation of a solar cell which, compared to the solar cell in Fig. 1, is provided with a second light absorbing layer 300. In alternative embodiments the second light absorbing layer 300 may be provided between the stack of layers 150 and the second electrode 140. The second light absorbing layer may comprise inorganic absorbers selected from the group of silicon (Si), copper-indium-gallium-diselenide (CIGS), cadmium-telluride (CdTe) and organic photovoltaic layer or a combination thereof.

Fig. 9 shows a solar cell comprising a first and a second stack of layers 150a, 150b provided between the first and the second electrode 120, 140. The first and the second stack of layers 150a, 150b may be provided like the stack of layers 150. In an alternative embodiment, the second stack of layers 150b may be provided between the first stack of layers 150a and the second electrode 140.

Fig. 10 shows a solar cell provided with a plurality of stacks of layers 150a, ..., 150c.

In an alternative embodiment which is shown in Fig. 11, between neighbours of the stacks of layers 150a, ..., 150c an interlayer 160a, 160b is provided.

Fig. 12 shows the current density (J) vs. voltage curves of the best-performing p-i-n solar cell device (example number 6) and the best-performing n-i-p solar cell device (example number 22). Both collar cells have the same cell area of 0.01 cm^2.

Fig. 13 shows the lifetime of a p-i-n solar cell device represented as open circuit voltage (V_{OC}) vs operating time (Time). It is evident that the solar cell with performance enhancement layer has stable V_{OC}. The solar cell without the performance enhancement layer shows a significant drop in V_{OC} after 100 hours.

Fig. 14 shows lifetime of a p-i-n solar cell device represented as power conversion efficiency (PCE) vs operating time (Time). The PCE vs Time is stable for p-type dopant concentrations above 6 mol%.

Fig. 15 shows lifetime of a p-i-n solar cell device represented as power conversion efficiency (PCE) vs operating time (Time). The PCE vs Time is most stable for n-type dopant concentrations of 30 mol%.

Following, experimental results with regard to the different embodiments of the solar cell shown in the figures are described.

Patterned ITO coated glass substrates are patterned by photolithography. Materials used are: p-type dopant 2,2'-(Perfluoronaphthalene-2,6-diylidene) dimalononitrile (F6-TCNNQ), first matrix compound N4,N4,N4",N4"-tetra([1,1'-biphenyl]-4-yl)-[1,1':4',1"-terphenyl]-4,4"-diamine (TaTm) and n-type dopant N1,N4-bis(tri-p-tolylphosphoranylidene)benzene-1,4-diamine (PhIm). The second matrix compound is fullerene (C60). The precursor materials for the perovskite light absorbing layer are PbI_2 and CH_3NH_3I (MAI).

With regard to characterization of the embodiments prepared, grazing incident X-ray diffraction (GIXRD) pattern are collected at room temperature on an Empyrean PANanalytical powder diffractometer using the Cu Kα1 radiation. Typically, three consecutive measurements are collected and averaged into single spectra. The surface morphology of the thin films is analyzed using atomic force microscopy (AFM, Multimode SPM, Veeco, USA). Scanning Electron Microscopy (SEM) images is performed on a Hitachi S-4800 microscope operating at an accelerating voltage of 2 kV over Platinum - metallized samples. Absorption spectra are collected using a fiber optics based Avantes Avaspec2048 Spectrometer.

Characterization of the solar cells is performed as follows: The external quantum efficiency (EQE) is estimated using the cell response at different wavelength (measured with a white light halogen lamp in combination with band-pass filters), where the solar spectrum mismatch is corrected using a calibrated Silicon reference cell (MiniSun simulator by ECN, the Netherlands).

The current density-voltage (J-V) characteristics are obtained using a Keithley 2400 source measure unit and under white light illumination, and the short circuit current density is corrected taking into account the device EQE. The electrical characterization was validated using a solar simulator by Abet Technologies (Model 10500 with an AM1.5G xenon lamp as the light source). Before each measurement, the exact light intensity is determined using a

calibrated Si reference diode equipped with an infrared cut-off filter (KG-3, Schott). The J-V curves are recorded between -0.2 and 1.2 V with 0.01V steps, integrating the signal for 20 ms after a 10 ms delay. This corresponds to a speed of about 0.3 V s^{-1}.

Different device layouts are used for the solar cells configurations: (1) four equal areas (0.0653 cm^2, defined as the overlap between the ITO and the top metal contact) and measured through a shadow masks with 0.01 cm^2 aperture, and (2) increasing areas (0.0897 cm^2, 0.1522 cm^2, 0.3541 cm^2 and 0.9524 cm^2) which is characterized by using a shadow mask with aperture areas of 0.0484 cm^2, 0.1024 cm^2, 0.2704 cm^2 and 0.8464 cm^2, respectively. For hysteresis study, different scan rates (0.1, 0.5 and 1 Vs^{-1}) are used, biasing the device from -0.2 to 1.2 V with 0.01 V steps and vice versa. Light intensity dependence measurements are done by placing 0.1, 1, 10, 20, 50% neutral density filters (LOT-QuantumDesign GmbH) between the light source and the device.

Further, with regard to device preparation, ITO-coated glass substrates are subsequently cleaned with soap, water and isopropanol in an ultrasonic bath, followed by UV-ozone treatment. They are transferred to a vacuum chamber integrated into a nitrogen-filled glovebox (MBraun, H_2O and O_2 < 0.1 ppm) and evacuated to a pressure of $1 \cdot 10^{-6}$ mbar. The vacuum chamber is equipped with six temperature controlled evaporation sources (Creaphys) fitted with ceramic crucibles. The sources are directed upwards with an angle of approximately 90° with respect to the bottom of the evaporator. The substrate holder to evaporation sources distance is approximately 20 cm. Three quartz crystal microbalance (QCM) sensors are used, two monitoring the deposition rate of each evaporation source and a third one close to the substrate holder monitoring the total deposition rate.

For thickness calibration, firstly the matrix compounds and the dopants (TaTm and F6-TCNNQ, C60 and PhIm) are individually sublimed. A calibration factor is obtained by comparing the thickness inferred from the QCM sensors with that measured with a mechanical profilometer (Ambios XP1). Then these materials are co-sublimed at temperatures ranging from 135-160 °C for the dopants to 250 °C for the matrix compounds, and the evaporation rate is controlled by separate QCM sensors and adjusted to obtain the desired doping concentration. In general, the deposition rate for TaTm and C60 is kept constant at 0.8 Å s^{-1}, while varying the deposition rate of the dopants during co-deposition. Undoped TaTm and C60 layers are deposited at a rate of 0.5 Å s^{-1}.

For the p-i-n configuration, 40 nm of the p-type doped first matrix layer (TaTm:F6-TCNNQ) capped with 10 nm of the pure TaTm are deposited. Once this deposition is completed, the chamber is vented with dry N_2 to replace the crucibles with those containing the precursor materials for the perovskite light absorbing layer deposition, PbI_2 and CH_3NH_3I. The vacuum chamber is evacuated again to a pressure of 10^{-6} mbar, and the perovskite films (light absorbing layer) are then obtained by co-deposition of the two precursors.

The calibration of the deposition rate for the CH_3NH_3I is difficult due to non-uniform layers and the soft nature of the material which impedes accurate thickness measurements. Hence, the source temperature of the CH_3NH_3I is kept constant at 70 °C and the CH_3NH_3I:PbI_2 ratio is controlled off line using grazing incident x-ray diffraction by adjusting the PbI_2 deposition temperature. The optimum deposition temperatures are 250 °C for the PbI_2 and 70 °C for the CH_3NH_3I. After deposition of a 500 nm thick perovskite film, the chamber is vented and the crucibles replaced with those containing C60 and PhIm, and evacuated again to a pressure of 10^{-6} mbar.

The solar cell devices are further processed by depositing a film of pure C60 and one of the n-type doped second matrix layer (C60:PhIm), with thicknesses of 10 and 40 nm, respectively. This process of exchanging crucibles is done to evaluate the effect of changes in the organic layer composition for an identical perovskite layer. In a single evaporation run five substrates (3 by 3 cm) are prepared, each substrate containing four cells. Generally, one substrate is reserved for a reference configuration allowing for evaluation of four variations in the matrix compound per perovskite evaporation. Finally the substrates are transferred to a second vacuum chamber where the metal electrode (100 nm thick) is deposited. For n-i-p devices, the same procedure as described before is used in the inverted order.

The devices prepared are listed in Table 1 (p-i-n layer sequence) and Table 2 (n-i-p layer sequence).

Table 1. Solar cells of the p-i-n layer sequence.

p-i-n Layer Sequence	Device Layer Stack	Device Stack
p-i-n (undoped reference)	TaTm/$MAPbI_3$/C60	A
p-i-n (two organic perfomance enhancement layers)	TaTm:F6-TCNNQ (x wt%)/TaTm/$MAPbI_3$/C60/C60:PhIm (30 wt%)	B p-type dopant x wt%

p-i-n (two organic perfomance enhancement layers)	TaTm:F6-TCNNQ (11 wt%)/TaTm/$MAPbI_3$/C60/C60:PhIm (x wt%)	B n-type dopant x wt%
p-i-n (two organic perfomance enhancement layers)	TaTm:F6-TCNNQ (11 wt%)/TaTm/$MAPbI_3$/C60/C60:PhIm (30 wt%)	B
p-i-n (no organic perfomance enhancement layer p-side)	TaTm:F6-TCNNQ (11 wt%)/$MAPbI_3$/C60/C60:PhIm (30 wt%)	E
p-i-n (no organic perfomance enhancement layer n-side)	TaTm:F6-TCNNQ (11 wt%)/TaTm/$MAPbI_3$/C60:PhIm (30 wt%)	F
p-i-n (two organic perfomance enhancement layers)	TaTm:F6-TCNNQ (11 wt%)/TaTm/$MAPbI_3$/C60/C60:PhIm (30 wt%)	B
p-i-n (no p-type layer, thin undoped layer)	TaTm (10nm) /$MAPbI_3$/C60/C60:PhIm (30 wt%)	G thin
p-i-n (no p-type layer, thick undoped layer)	TaTm(30nm)/$MAPbI_3$/C60/C60:PhIm (30 wt%)	G thick
p-i-n (no n-type layer, thin undoped layer)	TaTm:F6-TCNNQ (11 wt%)/TaTm/$MAPbI_3$/C60(10nm)	H thin
p-i-n (no n-type layer, thick undoped layer)	TaTm:F6-TCNNQ (11 wt%)/TaTm/$MAPbI_3$/C60(30nm)	H thick
p-i-n (two organic perfomance enhancement layers)	TaTm:F6-TCNNQ (11 wt%)/TaTm/$MAPbI_3$/C60/C60:PhIm (30 wt%)	B
p-i-n (n-type layer = bilayer dopant + n-type doped matrix)	TaTm:F6-TCNNQ (11 wt%)/TaTm/$MAPbI_3$/C60/PhIm/C60:PhIm (30 wt%)	J
p-i-n (n-type layer = bilayer n-type doped matrix + dopant)	TaTm:F6-TCNNQ (11 wt%)/TaTm/$MAPbI_3$/C60/C60:PhIm (30 wt%)/PhIm	K
p-i-n (thin pure p-	F6-TCNNQ (2 nm) /TaTm (48 nm)/ $MAPbI_3$	Q

dopant layer, one undoped layer)	(500 nm)/C60 (10 nm)/C60:PhIm (30 wt%) (40 nm)	

Table 2. Solar cells of the n-i-p layer sequence.

n-i-p Layer Sequence	Device Layer Stack	Device Stack
n-i-p (two organic perfomance enhancement layers)	C60:PhIm (x wt%)/C60/$MAPbI_3$/TaTm/TaTm:F6-TCNNQ (11 wt%)	L n-type dopant x wt%
n-i-p (two organic perfomance enhancement layers)	C60:PhIm (60 wt%)/C60/$MAPbI_3$/TaTm/TaTm:F6-TCNNQ (11 wt%)	M
n-i-p (no organic perfomance enhancement layer p-side)	C60:PhIm (60 wt%)/C60/$MAPbI_3$/TaTm:F6-TCNNQ (11 wt%)	N
n-i-p (no organic perfomance enhancement layer n-side)	C60:PhIm (60 wt%)/$MAPbI_3$/TaTm/TaTm:F6-TCNNQ (11 wt%)	O
n-i-p (alternative first organic matrix compound, alternative organic p-type dopant)	C60:PhIm (30wt%)/C60/ $MAPbI_3$/TaDi/TaDi:CyTa (11wt%)/	P
n-i-p (thin pure n-dopant layer, one undoped layer)	PhIm (2 nm)/C60 (48 nm)/ $MAPbI_3$ (500 nm)/TaTm (10 nm)/TaTm:F6-TCNNQ (11 wt%) (40 nm)	R
n-i-p (alternative metal n-type dopant)	C60:Yb (15 wt%) (40 nm)/C60 (10 nm)/$MAPbI_3$ (500 nm)/TaTm (10 nm)/TaTm:F6-TCNNQ (11 wt%)	S

For simplicity the layer sequences in the tables are written as text strings. The individual layers are separated by " / ". The compounds comprised by the layer are given in the text. For dopants the concentration is give in brackets "( )" in weight percent (wt%). The layer sequence in the solar cell device is subsequently called "stack".

The perovskite light absorbing layers are used to prepare planar diodes by sandwiching a 500 nm thick perovskite layer between organic p-type layer (hole transport or hole injection layers) and n-type layer (electron transport or electron injection layers).

In order to compare the solar cells to a reference, a device with undoped layers is chosen as a reference solar cell. This reference device with undoped charge transport layers 230, 240 is shown in Fig. 2.

For comparison of the different solar cells four parameters are selected, which are defined as follows (source: www.pveducation.org):

1) Open circuit voltage (Voc) in mV - maximum voltage available from a solar cell, and this occurs at zero current
2) Short circuit current (Jsc) in mA cm^{-2} - current through the solar cell when the voltage across the solar cell is zero (i.e., when the solar cell is short circuited). This is the largest current which may be drawn from the solar cell.
3) At both of these operating points, Voc and Jsc, the power from the solar cell is zero. The "fill factor" (FF) in %, is a parameter which, in conjunction with Voc and Isc, determines the maximum power from a solar cell. The FF is defined as the ratio of the maximum power from the solar cell to the product of Voc and Isc. Graphically, the FF is a measure of the "squareness" of the solar cell and is also the area of the largest rectangle which will fit in the IV curve.
4) Power conversion efficiency (PCE) in % - ratio of energy output from the solar cell to input energy from the sun. PCE = Voc * Jsc * FF

The performance parameters are measured on 0.01 cm^2 solar cells for examples 1 to 15, on 0.0264 cm^2 for examples 16 to 22 and on 0.1 cm^2 for sample 23.

EXPERIMENT 1. The parameters of the solar cells prepared are compared to a reference solar cell not comprising any electric dopant or electrically doped layers. The architecture of such device in p-i-n layer sequence is shown in Fig. 1a. As an undoped layer the first matrix compound is used between first electrode and light absorbing layer and the second matrix compound is used between the second electrode and the light absorbing layer.

Using the architecture described above, employing single layers of undoped charge transport layers, the photovoltaic performance of the diodes under 1 sun illumination (1 sun corresponds to standard illumination at AM1.5, or 1 kW/m^2) is poor, due to a pronounced s-

shape of the current density (*J*) versus voltage (*V*) curve (not shown). This leads to low fill factors (*FF*) and hence low PCE values (Table 3). This indicates that the extraction of the charge carrier's generated in the light absorbing layer is severely hindered.

Table 3. Performance parameters of comparative example number 1, the undoped reference solar cell device stack A (see Fig. 2).

Comparative Example Number	Device Stack Abbreviation		JSC ($mAcm^{-2}$)	VOC (mV)	FF (%)	PCE (%)
1	A		20.12	1041	16.8	3.5

The present disclosure is the insertion of p-doped and n-doped layers on either side of the light absorbing layer. These doped layers are either single layers or multiple layers. In order to study the effect of the doped layers on the solar cell device performance several device stack variations are tested in experiments 2 to 8.

EXPERIMENT 2. Variations of the concentration of the p-type dopant in the first matrix compound are performed at constant concentration of the n-type dopant of 30wt%. The optimum concentration of p-type dopant is 11 wt% (Table 4).

EXPERIMENT 3. Variations of the concentration of the n-type dopant in the second matrix compound are performed at constant concentration of the p-type dopant of 11wt%. The optimum concentration of n-type dopant is 30 wt% (Table 5).

Table 4. Performance parameters of solar cell device stack B with different concentrations of p-type dopant.

Example Number	Device Stack		JSC ($mAcm^{-2}$)	VOC (mV)	FF (%)	PCE (%)
2	B	3 wt% F6-TCNNQ	21.37	1053	56.8	12.78
3	B	5 wt% F6-TCNNQ	20.11	1065	62.7	13.43
4	B	6 wt% F6-TCNNQ	20.35	1085	64	14.13
5	B	9 wt% F6-TCNNQ	19.29	1084	72.1	15.02

6	B	11 wt% F6-TCNNQ	20.02	1082	73.5	15.92
7	B	15 wt% F6-TCNNQ	18.88	1081	71.9	14.67
8	B	20 wt% F6-TCNNQ	19.43	1084	72.4	15.25
9	B	40 wt% F6-TCNNQ	19.31	1055	73.8	15.02

Table 5. Performance parameters of solar cell device stack B with different concentrations of n-type dopant.

Example Number	Device Stack Abbreviation		JSC ($mAcm^{-2}$)	VOC (mV)	FF (%)	PCE (%)
10	B	15 wt% PhIm	18.89	1095.04	68.82	14.23
11	B	30 wt% PhIm	18.84	1082.41	72.34	14.75
12	B	45 wt% PhIm	19.97	1110.1	66.26	14.68
13	B	60 wt% PhIm	18.73	1082.97	68.27	13.84

Table 6. Performance parameters of solar cell device stack B.

Example Number	Device Stack		JSC ($mAcm^{-2}$)	VOC (mV)	FF (%)	PCE (%)
6	B	11 wt% p-type dopant 30wt% n-type dopant	20.02	1082	73.5	15.92

The best performing p-i-n device stack B comprises a p-type layer containing 11wt% p-dopant and an n-type layer containing 30wt% n-type dopant and containing an undoped organic performance enhancement layer on either side of the light absorbing layer and in direct contact with the light absorbing layer (Table 6). FF and PCE are largely improved compared to the undoped reference cell device stack A, comparative example number 1.

EXPERIMENT 4. The effect of the undoped organic performance enhancement layer is tested. The undoped organic performance enhancement layer is inserted between the light absorbing layer and the p-type layer and/or between the light absorbing layer and the n-type

layer. Leaving out the undoped organic performance enhancement layer between the light absorbing layer and the n-type layer significantly reduces the device performance. Leaving out the undoped organic performance enhancement layer between the light absorbing layer and the p-type layer has no significant effect on the device performance (Table 7). An investigation of the lifetime of the solar cell shows that the undoped organic performance enhancement layer in example number 6 is improving the lifetime when compared to example number 15 without undoped organic performance enhancement layer (Fig. 13).

Table 7. Performance parameters of p-i-n solar cell device stack E and F.

Example Number	Device Stack		JSC ($mAcm^{-2}$)	VOC (mV)	FF (%)	PCE (%)
14	E	no perfomance enhancement layer p-side	20.19	1033	73.3	15.3
15	F	no perfomance enhancement layer n-side	17.82	1032	45	8.3

EXPERIMENT 5. In solar cell device stacks G and H the effect of leaving out either the p-type layer or the n-type layer is tested. As an undoped layer the first matrix compound is used between first electrode and light absorbing layer and the second matrix compound is used between the second electrode and the light absorbing layer. The thickness of the undoped layer is 10 nm (thin) and 30 nm (thick). Table 8 shows that the solar cell performance is significantly reduced if either p-type layer or n-type layer are not used.

Table 8. Performance parameters of p-i-n solar cell device stack G and H (thin and thick).

Example Number	Device Stack		JSC ($mAcm^{-2}$)	VOC (mV)	FF (%)	PCE (%)
16	G thin	no p-type layer	21.13	994	28	5.87
17	G thick	no p-type layer	21.25	1040	42.3	9.36
18	H thin	no n-type layer	9.14	942	43.4	3.73
19	H thick	no n-type layer	19.39	1116	54	11.68

EXPERIMENT 6. The solar cell device stack option of n-type layer consisting of a pure dopant layer as well as of a layer comprising the n-type dopant and the second matrix compound is tested in two configurations: configuration J with the n-type dopant layer inserted between the undoped organic performance enhancement layer and the layer comprising the n-type dopant and the second matrix compound and configuration K with the n-type dopant layer inserted between the layer comprising the n-type dopant and the second matrix compound and the second electrode. Table 9 shows solar cell performance data of solar cell device stacks J and K.

Table 9. Performance parameters of p-i-n solar cell device stack J and K.

Example Number	Device Stack		JSC ($mAcm^{-2}$)	VOC (mV)	FF (%)	PCE (%)
20	J		19.55	1097	70.1	15.03
21	K		18.6	1054	49.2	9.65

The use of the pure n-type dopant layer in configuration J shows better solar cell device performance.

EXPERIMENT 7. Solar cells in n-i-p layer sequence (Fig. 1b) are tested using the optimum concentrations of organic p-type dopant (11 wt%) and n-type dopant (30 wt%) of example 6. The performance parameters of the solar cells are shown in Table 10.

Table 10. Comparison of performance parameters of solar cell device stack L (n-i-p layer sequence) to solar cell device stack B (p-i-n layer sequence).

Example Number	Device Stack		JSC ($mAcm^{-2}$)	VOC (mV)	FF (%)	PCE (%)
22	L (0.01 cm2 cell area)	11 wt% p-type dopant 30wt% n-type dopant	19.32	1108	81.6	17.46
23	M (0.1 cm2 cell area)	11 wt% p-type dopant 30wt% n-type dopant	22.08	1141	80.5	20.30
6	B	11 wt% p-type dopant	20.02	1082	73.5	15.92

		30wt% n-type dopant				

The solar cell device stack L (n-i-p layer sequence) shows better FF and PCE in comparison to the solar cell device stack B (p-i-n layer sequence). The solar cell of stack M (0.1 cm^2 cell area) has a higher PCE compared to the solar cell of stack L (0.01 cm^2 cell area). The current-voltage curves of the examples number 6 and 22 are shown in Fig. 12.

EXPERIMENT 8. Solar cells in n-i-p layer sequence (Fig. 1b) are tested using the alternative first matrix compound TaDi with a first oxidation potential about 0.09 V above the first oxidation potential of the light absorbing layer. And the alternative organic p-dopant CyTa having about the same first reduction potential as F6TCNNQ. The solar cell performance very similar when using a first matrix compound which has a first oxidation potential about 0,09 V more positive than the light absorbing layer material.

Table 11. Performance parameters of n-i-p solar cell device stack J and P.

Example Number	Device Stack		J_{SC} ($mAcm^{-2}$)	V_{OC} (mV)	FF (%)	PCE (%)
22	J	11 wt% F6TCNNQ in TaTm	19.32	1108	81.6	17.46
24	P	11 wt% CyTa in TaDi	20.20	1070	76.0	16.30

In conclusion, a substantial increase in performance, lifetime and / or fill factor has been achieved over the state of the art.

Following, further alternative embodiments of solar cells are described.

A solar cell of the p-i-n layer sequence provided with a device stack identified by "Example number 25" (see Table 14) was prepared.

Table 12. Performance parameters of solar cell of the p-i-n layer sequence with neat p-type dopant layer (example number 25).

Example Number	Device Stack		JSC ($mAcm^{-2}$)	VOC (mV)	FF (%)	PCE (%)
25	Q	F6-TCNNQ (2 nm)	18.60	1027	53.4	10.2

Solar cell of the n-i-p layer sequence provided with a device stack identified by "Example numbers 26 and 27" (see Table 15) were prepared.

Table 13. Performance parameters of solar cell of the n-i-p layer sequence with neat n-type dopant layer (Example number 26) and with metal-n-type dopant as n-type dopant in n-type layer (Example number 27).

Example Number	Device Stack		JSC ($mAcm^{-2}$)	VOC (mV)	FF (%)	PCE (%)
26	R	PhIm (2 nm)	20,84	1097	76,0	17,4
27	S	C60:Yb (15 wt%) (40 nm)	19,27	1031	71,2	14,1

In another aspect, the solar cell may be part of a larger photovoltaic device.

Table 14. Energy levels of materials used in examples.

Compound Name	Ionization Potential	First Oxidation Potential	First Reduction Potential
TaTm	-5.39 eV (AC-2)	0.40 V (vs ferrocene in dichloromethane)	
F6-TCNNQ			0.25 V (vs ferrocene in acetonitrile)
$MAPbI_3$	-5.40 eV *		
C60			-1.00 V **
PhIm		- 0.46 V (vs ferrocene in dichloromethane)	

TaDi	-5.76 eV (AC-3)	0.49 V (vs ferrocene in dichloromethane)	
CyTa			0.25 V (vs ferrocene in acetonitrile)

* Ionization potential MaPbI3 taken from Energies 2016, 9(11), 861.

** For cyclic voltammetry data see: Reed, Bolskar, Chem. Rev. 100, 1075 (2000); Ered ca. -1V vs Fc/Fc+ (Table 1), cf. table 2 regarding variability of reduction potential in various solvent.

Referring to Table 14, the ionization potential of the materials applied is >5.30eV.

The features disclosed in this specification, the figures and / or the claims may be material for the realization of various embodiments, taken in isolation or in various combinations thereof.

Claims

1. A solar cell, comprising
   - a first electrode;
   - a second electrode; and
   - at least one stack of layers provided between the first electrode and the second electrode, the at least one stack of layers comprising
     - a first light absorbing layer provided with a layer thickness of about 200 nm to about 700 nm, and comprising an absorber compound provided with a perovskite crystal structure;
     - a first organic p-type layer provided between the first electrode and the first light absorbing layer, the first organic p-type layer comprising at least one of
       - a layer comprising an organic p-type dopant; and
       - a layer comprising a mixture of an organic p-type dopant and a first organic aromatic matrix compound;

       wherein, for the first organic p-type layer, the following is provided:
       - the first organic aromatic matrix compound has a molecular weight of about 400 to about 1500;
       - the organic p-type dopant has a molecular weight of about 350 to about 1700;
       - the oxidation potential of the first organic aromatic matrix compound is equal to or less negative compared to N2,N2,N2',N2',N7,N7,N7',N7'-octakis(4-methoxyphenyl)-9,9'-spirobi[fluorene]-2,2',7,7'-tetraamine and equal or less positive than 1,3-bis(carbazol-9-yl)benzene when measured under the same conditions by cyclic voltammetry against Fc/Fc^+ in dichloromethane solution; and
       - the reduction potential of the organic p-type dopant is equal to or more positive compared to 2,3,5,6-Tetrafluor-7,7,8,8-tetracyanochinodimethan when measured by cyclic voltammetry against Fc/Fc^+ in acetonitrile; and
     - a first n-type layer provided between the second electrode and the first light absorbing layer, the first n-type layer comprising at least one of
       - a layer comprising an n-type dopant; and
       - a layer comprising of a mixture of an n-type dopant and a second organic aromatic matrix compound;

       wherein, for the first n-type layer, the following is provided:
       - the second organic aromatic matrix compound has a molecular weight of about 300 to about 1500; and

- the reduction potential of the second organic aromatic matrix compound is in the range of about ± 1.0 V, preferably ± 0.5 V, compared to the reduction potential of C_{60} when measured under the same conditions by cyclic voltammetry against Fc/Fc^+ in acetonitrile; and
- the n-type dopant is one of
  - a molecular dopant comprising an organic compound having a molecular weight of about 300 to about 1500, and
  - a metal dopant selected from the group consisting of a metal halide having a molecular weight of about 25 to about 500, a metal complex having a molecular weight of about 150 to about 1500, and a zero-valent metal selected from the group consisting of alkali metal, alkaline earth metal, and rare earth metals.

2. The solar cell according to claim 1, wherein the absorber compound has a stoichiometry of AMX_3 or A_2MX_4, where "A" and "M" are cations and "X" is an anion.

3. The solar cell according to claim 1 or 2, wherein the at least one stack of layers further comprises at least one of
   - a first undoped organic performance enhancement layer arranged between the organic p-type layer and the first light absorbing layer; and
   - a second undoped organic performance enhancement layer arranged between the organic n-type layer and the first light absorbing layer.

4. The solar cell according to any of the preceding claims, further comprising at least one of
   - a second n-type layer provided between the first electrode and the at least one stack of layers; and
   - a second organic p-type layer provided between the at least one stack of layers and the second electrode.

5. The solar cell according to any one of the preceding claims, further comprising a second light absorbing layer arranged between the first stack of layers and one of the first and the second electrode.

6. The solar cell according to any of the preceding claims, comprising at least two stacks of layers arranged between the first and the second electrode.

7. The solar cell according to at least one of the preceding claims, wherein the first organic aromatic matrix compound is selected from the group consisting of triarylamine, carbazole, thiophene, phthalocyanine, diphenylhydrazone, and quinoxaline.

8. The solar cell according to at least one of the preceding claims, wherein the second organic aromatic matrix compound is selected from the group consisting of acridine, benzoacridine, dibenzoacridine, anthracene, pyrene, triazine, and xanthene.

9. The solar cell according to at least one of the preceding claims, wherein the oxidation potential of the n-type dopant is equal or less positive than (1,3-dicyclohexyl-4,5-dimethyl-1H-imidazol-3-ium-2-yl)triphenylborate when measured under the same conditions by one of cyclic voltammetry against Fc/Fc^+ in dichloromethane solution.

10. The solar cell according to at least one of the preceding claims, wherein the n-type dopant is one of an alkali halide, and a metal complex selected from the group consisting of an alkali metal organic complex and main group and transition metal paddle-wheel complexes.

11. The solar cell according to at least one of the preceding claims, wherein the organic p-type dopant is provided with a concentration of about 3 wt% to about 50 wt% in the organic p-type layer.

12. The solar cell according to at least one of the preceding claims, wherein the n-type dopant in the n-type layer is provided with a concentration of
    - in case of a molecular dopant, about 3 wt% to about 60 wt%, and
    - in case of a metal dopant, about 0.5 mol% to about 10 mol%.

13. The solar cell according to at least one of the preceding claims, wherein in the at least one stack of layers, at least one of the following is provided:
    - the organic p-type layer is having a layer thickness of about 25 nm to about 1000 nm, preferably 30 to 500 nm;
    - the n-type layer is having a layer thickness of about 25 nm to about 1000 nm, preferably 30 to 500 nm; and
    - the undoped organic performance enhancement layer is having a layer thickness of about 5 nm to about 30 nm.

14. The solar cell according to at least one of the preceding claims, wherein the reduction potential of the organic p-type dopant is equal or more positive compared to 2,2'-(perfluoronaphthalene-2,6-diylidene)dimalononitrile when measured by cyclic voltammetry against Fc/Fc^+ in acetonitrile.

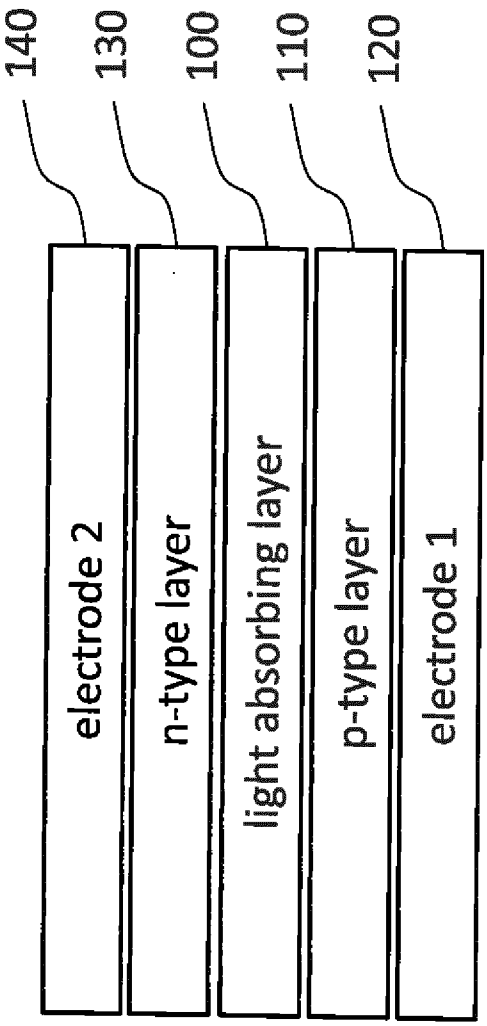
140
130
100
110
120
First stack of layers 150
p-i-n layer sequence
electrode 2
n-type layer
light absorbing layer
p-type layer
electrode 1

Fig. 1a

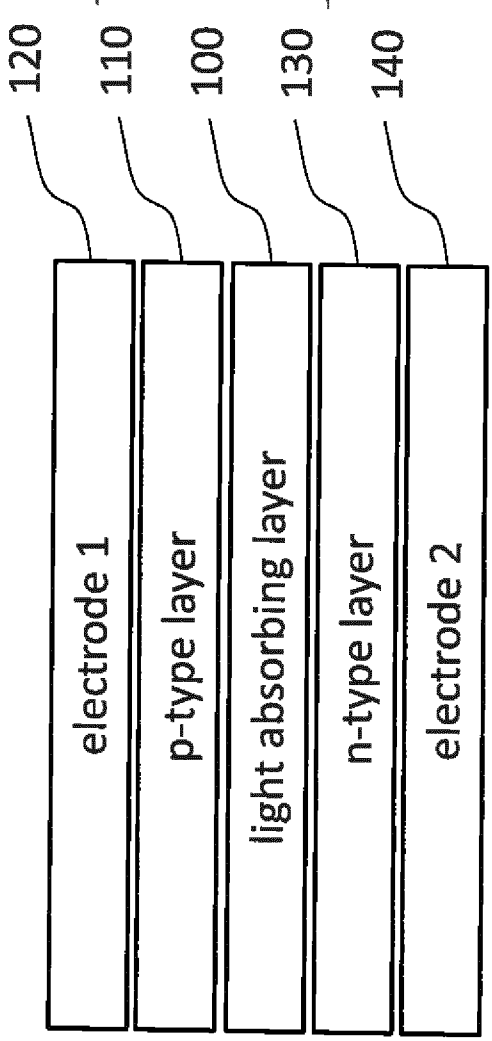
120
110
100
130
140
First stack of layers 150
n-i-p layer sequence
electrode 1
p-type layer
light absorbing layer
n-type layer
electrode 2

Fig. 1b

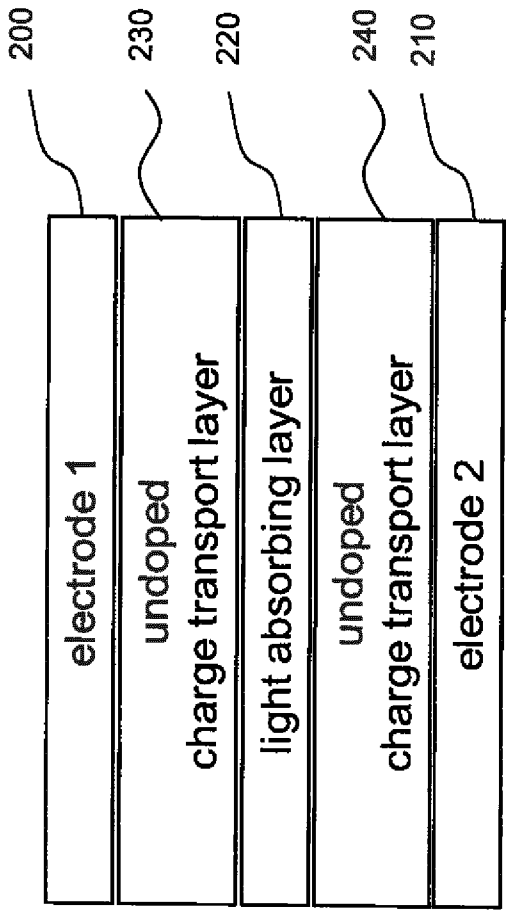
200
230
220
240
210
electrode 1
undoped
charge transport layer
light absorbing layer
undoped
charge transport layer
electrode 2

Fig. 2

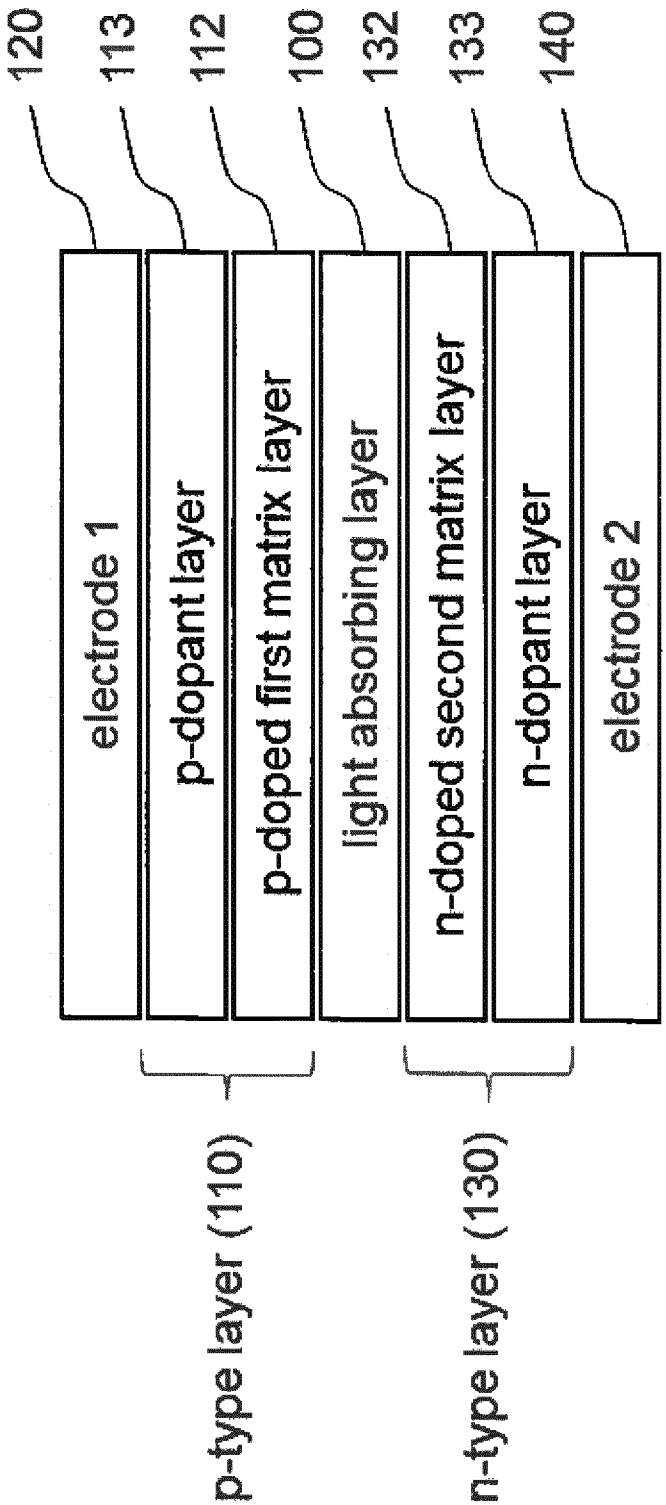
120
113
112
100
132
133
140
electrode 1
p-dopant layer
p-doped first matrix layer
light absorbing layer
n-doped second matrix layer
n-dopant layer
electrode 2
p-type layer (110)
n-type layer (130)

Fig. 3

Fig. 4

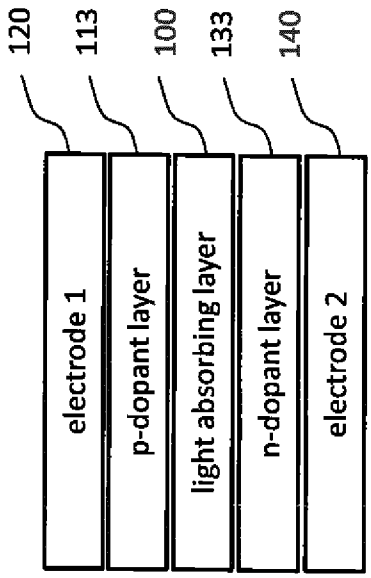
120
113
100
133
140
electrode 1
p-dopant layer
light absorbing layer
n-dopant layer
electrode 2

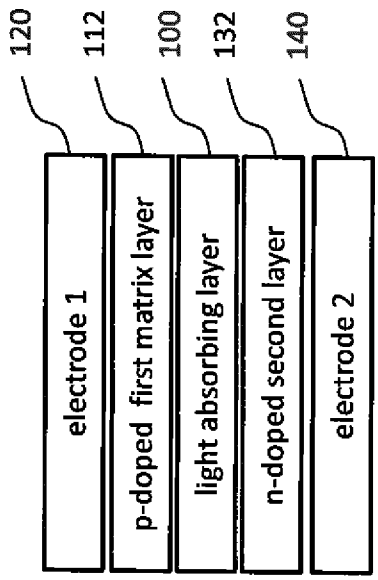
120
112
100
132
140
electrode 1
p-doped first matrix layer
light absorbing layer
n-doped second layer
electrode 2

Fig. 5

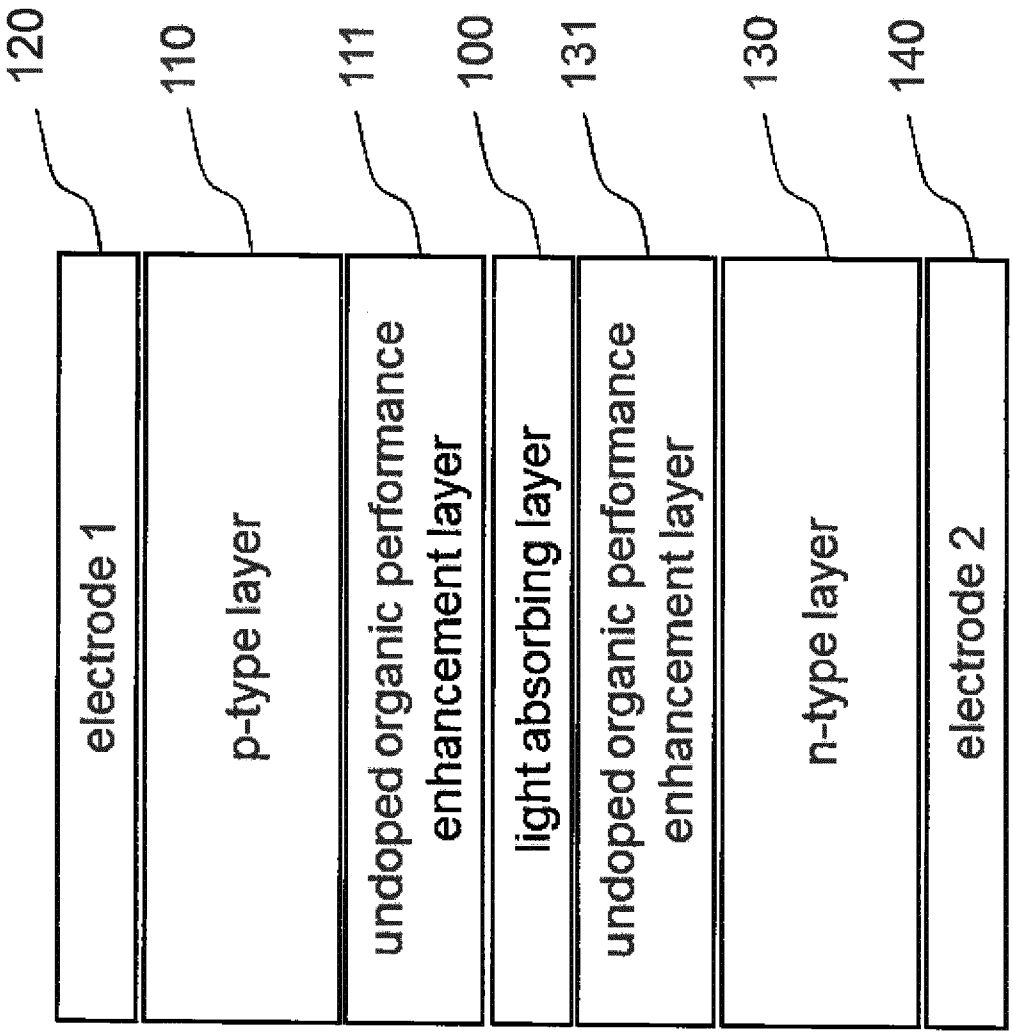
120
110
111
100
131
130
140
electrode 1
p-type layer
undoped organic performance enhancement layer
light absorbing layer
undoped organic performance enhancement layer
n-type layer
electrode 2

Fig. 6

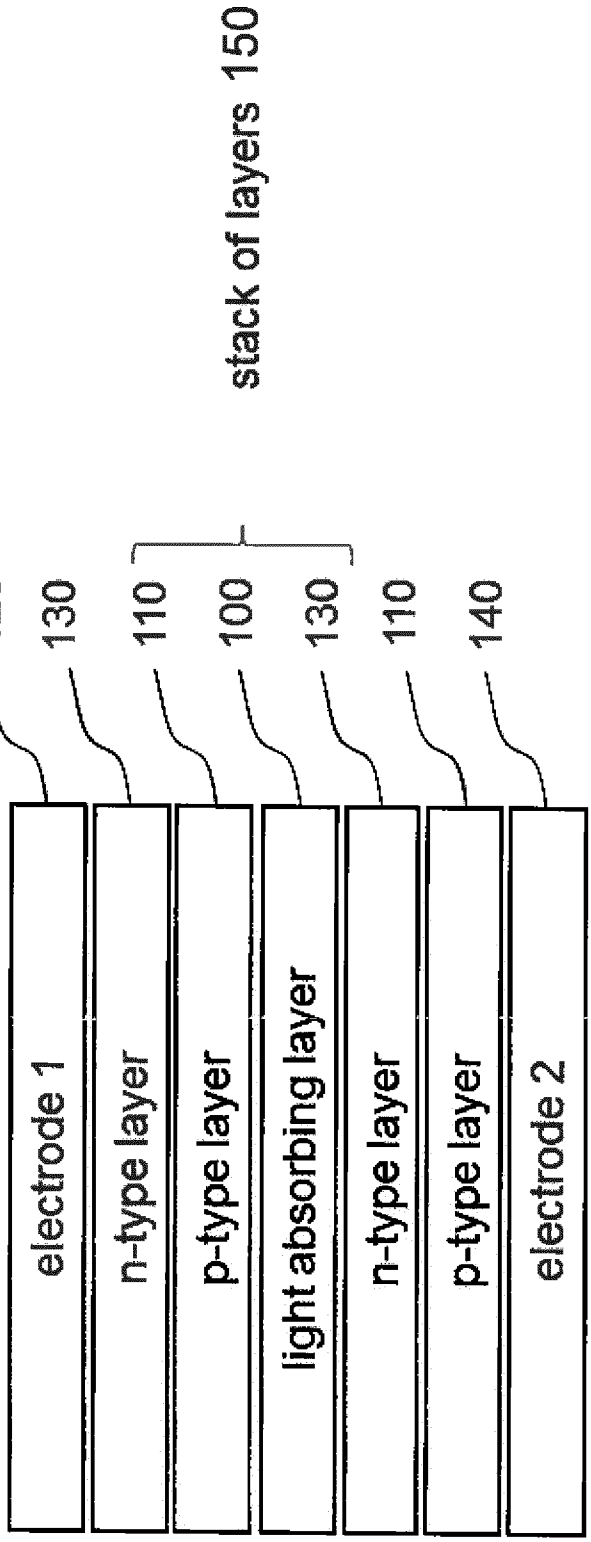
stack of layers 150
120
130
110
100
130
110
140
electrode 1
n-type layer
p-type layer
light absorbing layer
n-type layer
p-type layer
electrode 2

Fig. 7

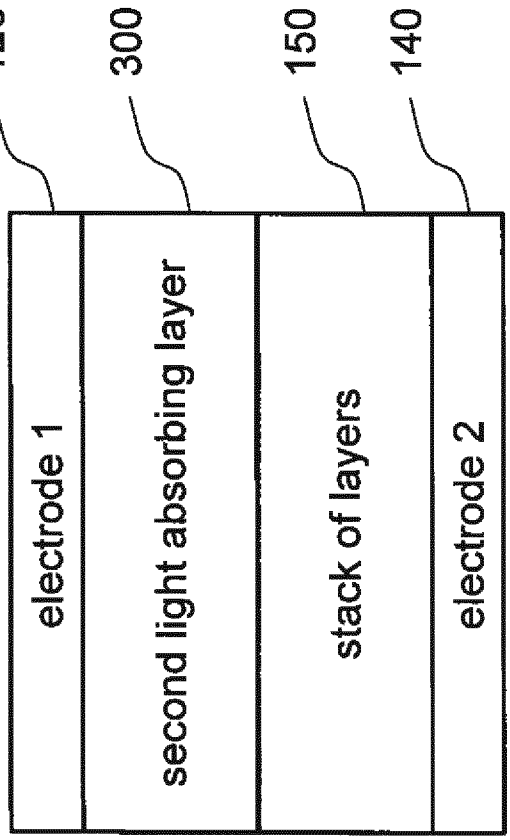
120
300
150
140
electrode 1
second light absorbing layer
stack of layers
electrode 2

Fig. 8

Fig. 9

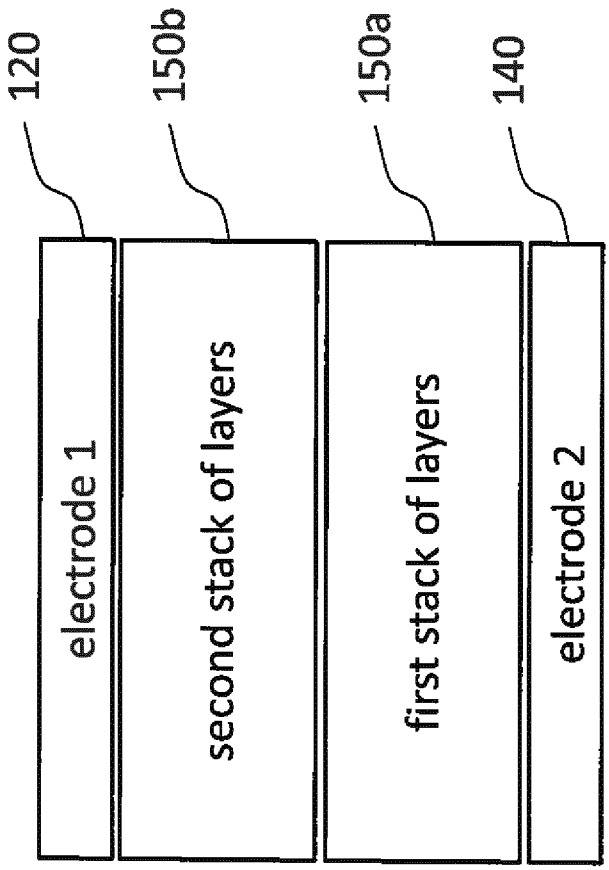
120
150b
150a
140
electrode 1
second stack of layers
first stack of layers
electrode 2

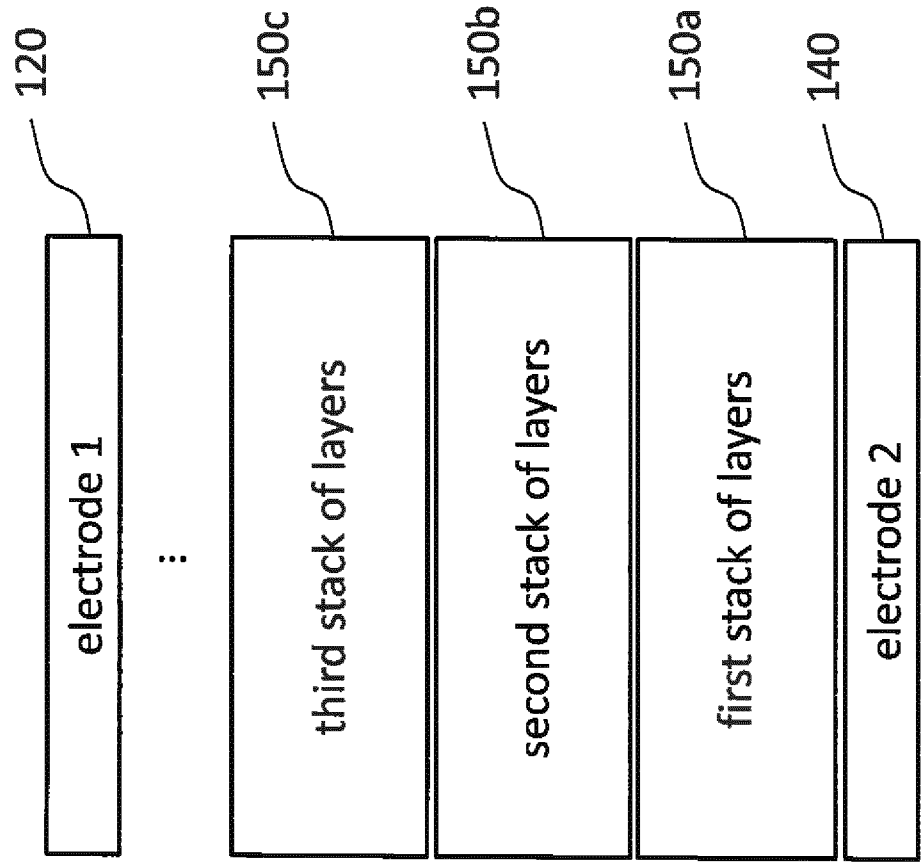
120
150c
150b
150a
140
electrode 1
:
third stack of layers
second stack of layers
first stack of layers
electrode 2

Fig. 10

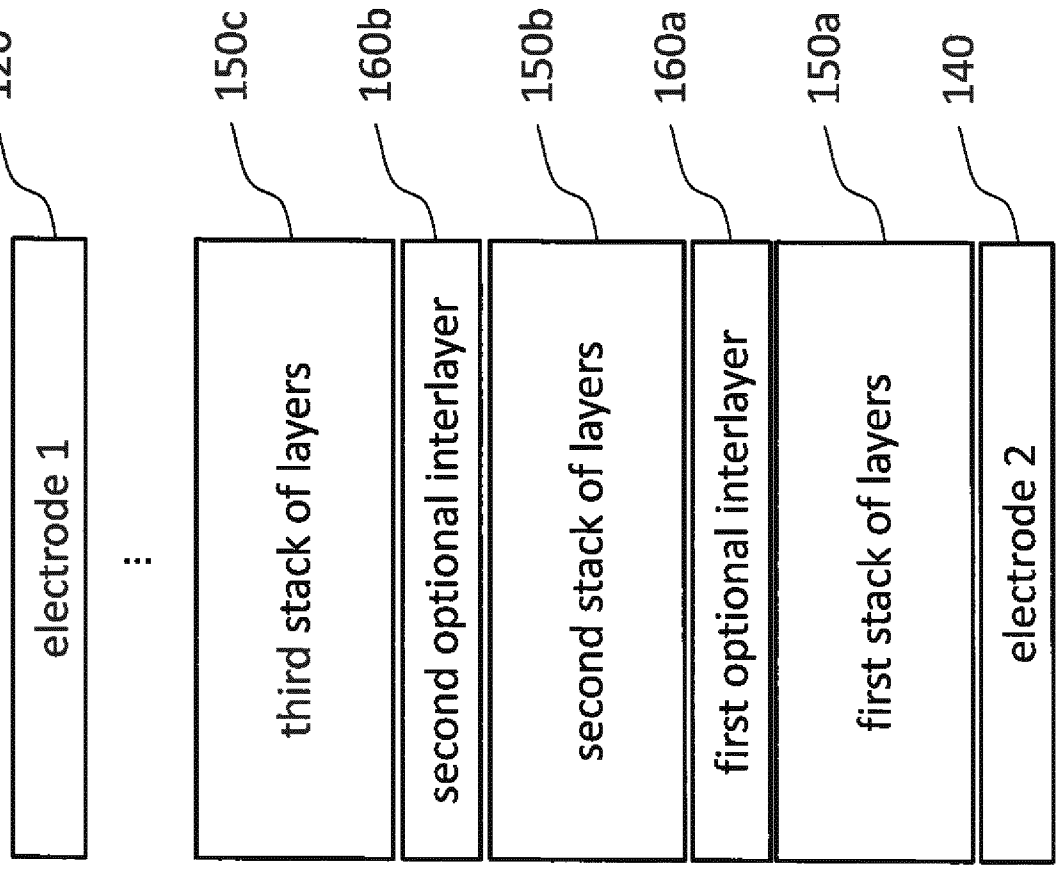
120
150c
160b
150b
160a
150a
140
electrode 1
:
third stack of layers
second optional interlayer
second stack of layers
first optional interlayer
first stack of layers
electrode 2

Fig. 11

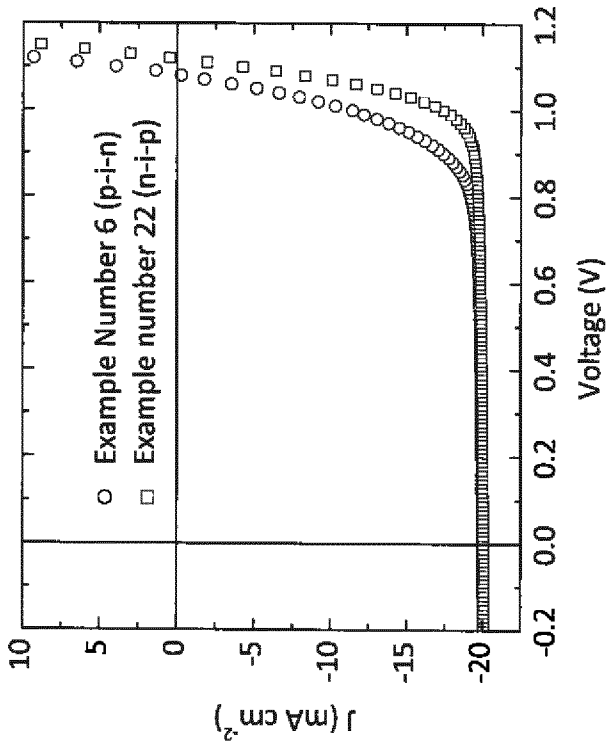
Example Number 6 (p-i-n)
Example number 22 (n-i-p)
J (mA cm⁻²)
Voltage (V)
10
5
0
-5
-10
-15
-20
-0.2
0.0
0.2
0.4
0.6
0.8
1.0
1.2

Fig. 12

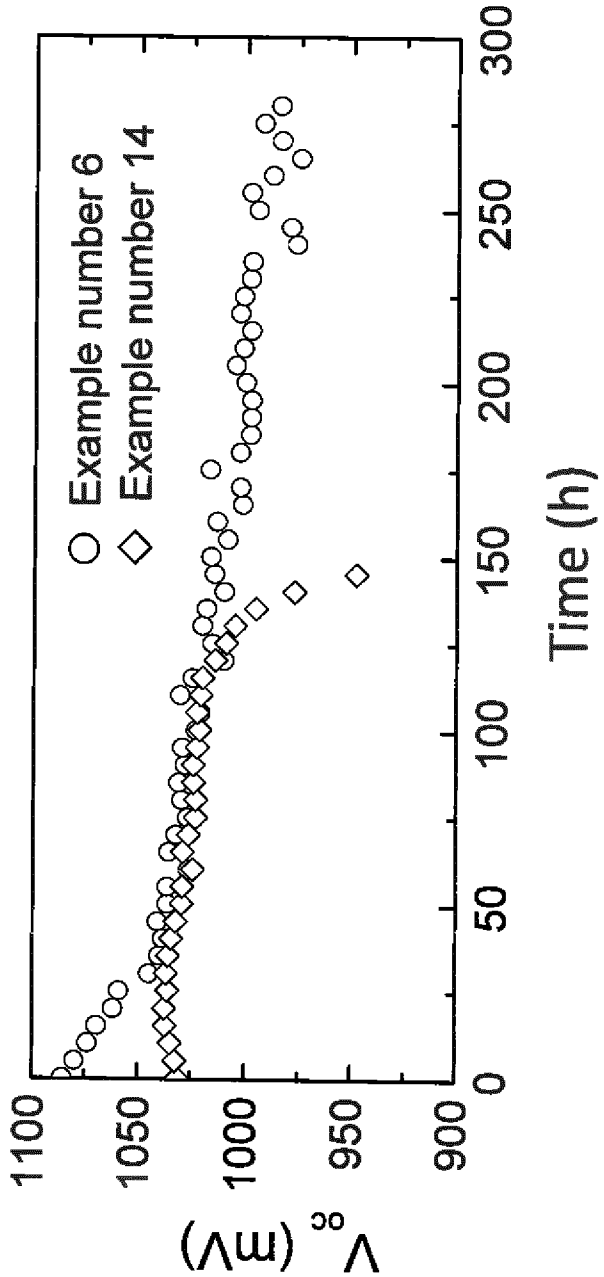
Example number 6
Example number 14
V_{oc} (mV)
Time (h)
1100
1050
1000
950
900
0
50
100
150
200
250
300

Fig. 13

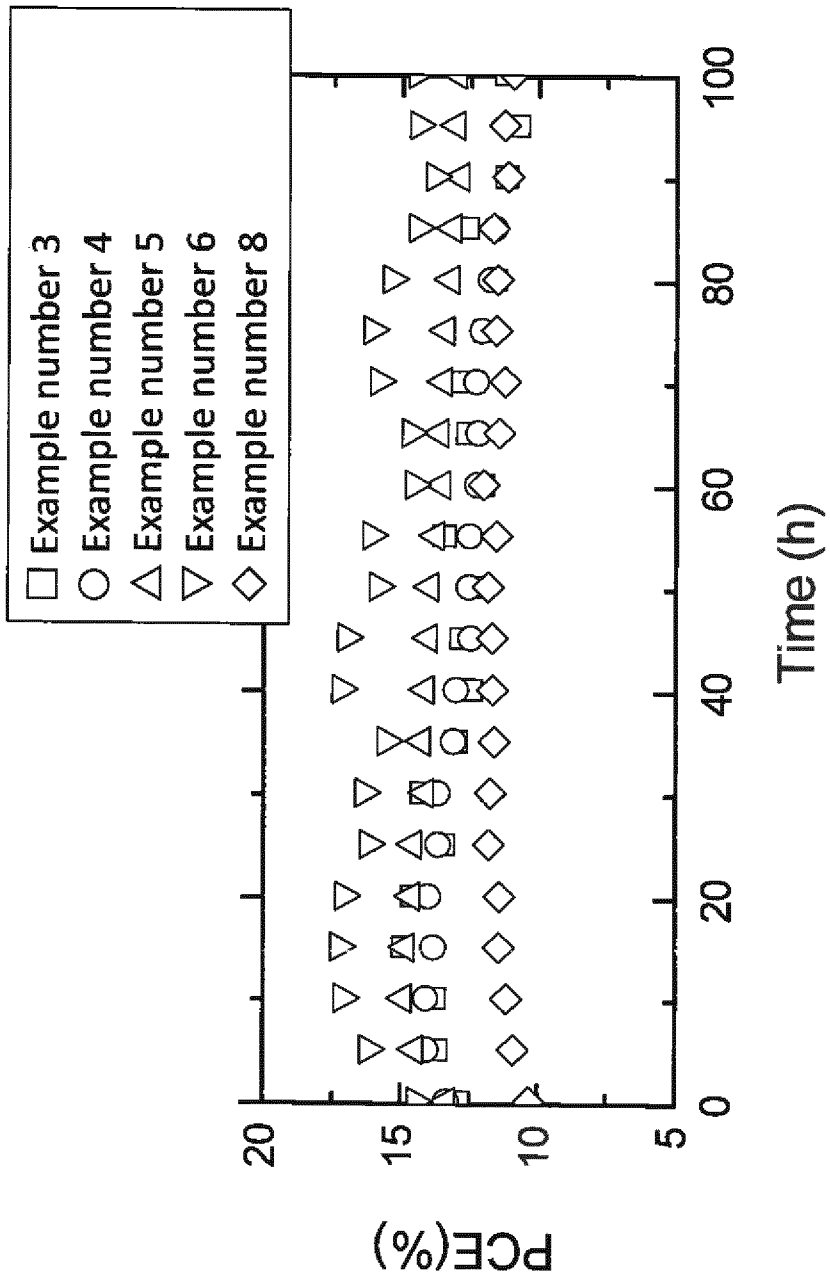
Example number 3
Example number 4
Example number 5
Example number 6
Example number 8
PCE(%)
20
15
10
5
0
20
40
60
80
100
Time (h)

Fig. 14

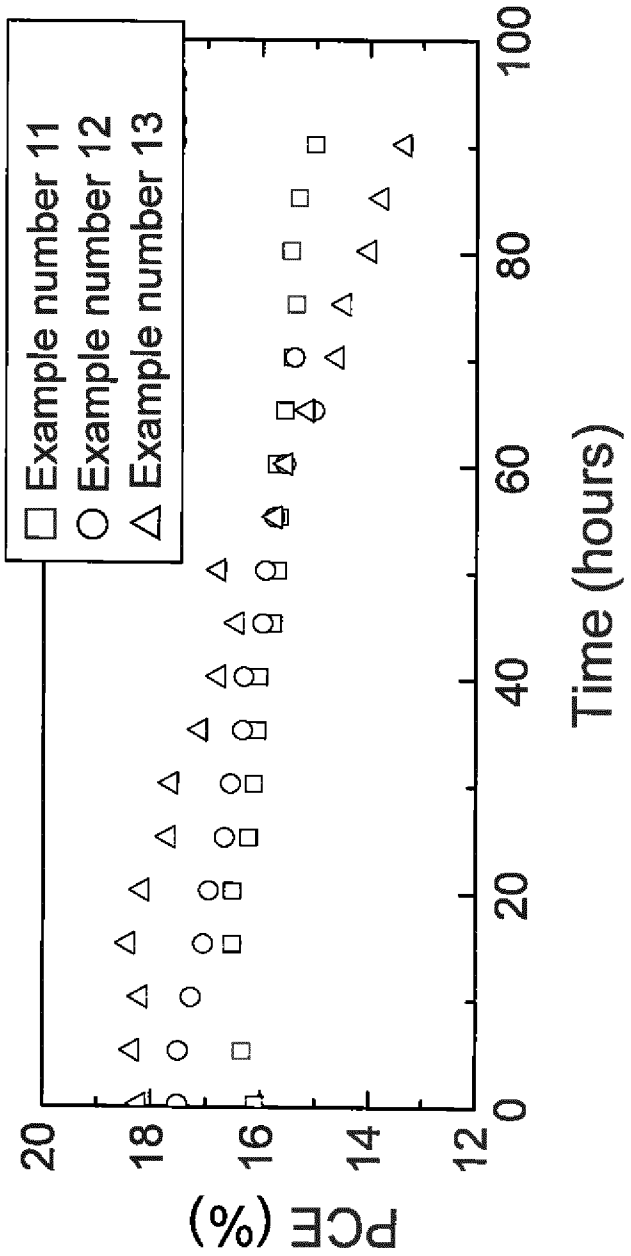
Example number 11
Example number 12
Example number 13
PCE (%)
20
18
16
14
12
0
20
40
60
80
100
Time (hours)

Fig. 15

INTERNATIONAL SEARCH REPORT

International application No
PCT/EP2017/060675

A. CLASSIFICATION OF SUBJECT MATTER
INV. H01L51/42 H01L27/30
ADD.

According to International Patent Classification (IPC) or to both national classification and IPC

B. FIELDS SEARCHED

Minimum documentation searched (classification system followed by classification symbols)
H01L

Documentation searched other than minimum documentation to the extent that such documents are included in the fields searched

Electronic data base consulted during the international search (name of data base and, where practicable, search terms used)
EPO-Internal

C. DOCUMENTS CONSIDERED TO BE RELEVANT

Category*	Citation of document, with indication, where appropriate, of the relevant passages	Relevant to claim No.
Y	LAUREN E. POLANDER ET AL: "Hole-transport material variation in fully vacuum deposited perovskite solar cells", APL MATERIALS, vol. 2, no. 8, 14 July 2014 (2014-07-14), page 081503, XP055315493, DOI: 10.1063/1.4889843 pages 081503-2, line 17 - pages 081503-3, line 38; figure 1 -----	1-14
Y	WO 2012/175219 A1 (NOVALED AG [DE]; DOROK SASCHA [DE]; HEGGEMANN ULRICH [DE]; FALTIN INA) 27 December 2012 (2012-12-27) page 25, line 8 - page 26, line 20; example Device 3 page 11; compound 4 ----- -/--	1-14

[X] Further documents are listed in the continuation of Box C.

[X] See patent family annex.

* Special categories of cited documents :

"A" document defining the general state of the art which is not considered to be of particular relevance

"E" earlier application or patent but published on or after the international filing date

"L" document which may throw doubts on priority claim(s) or which is cited to establish the publication date of another citation or other special reason (as specified)

"O" document referring to an oral disclosure, use, exhibition or other means

"P" document published prior to the international filing date but later than the priority date claimed

"T" later document published after the international filing date or priority date and not in conflict with the application but cited to understand the principle or theory underlying the invention

"X" document of particular relevance; the claimed invention cannot be considered novel or cannot be considered to involve an inventive step when the document is taken alone

"Y" document of particular relevance; the claimed invention cannot be considered to involve an inventive step when the document is combined with one or more other such documents, such combination being obvious to a person skilled in the art

"&" document member of the same patent family

Date of the actual completion of the international search	Date of mailing of the international search report
27 June 2017	05/07/2017

Name and mailing address of the ISA/	Authorized officer
European Patent Office, P.B. 5818 Patentlaan 2 NL - 2280 HV Rijswijk Tel. (+31-70) 340-2040, Fax: (+31-70) 340-3016	Fratiloiu, Silvia

1

Form PCT/ISA/210 (second sheet) (April 2005)

INTERNATIONAL SEARCH REPORT

International application No
PCT/EP2017/060675

C(Continuation). DOCUMENTS CONSIDERED TO BE RELEVANT

Category*	Citation of document, with indication, where appropriate, of the relevant passages	Relevant to claim No.
A	EP 2 942 826 A2 (TECH UNIVERSITÄT DRESDEN [DE]) 11 November 2015 (2015-11-11) cited in the application example 2 -----	1-14

1

INTERNATIONAL SEARCH REPORT

Information on patent family members

International application No
PCT/EP2017/060675

Patent document cited in search report	Publication date	Patent family member(s)	Publication date
WO 2012175219 A1	27-12-2012	CN 103765621 A	30-04-2014
		EP 2724388 A1	30-04-2014
		JP 2014524142 A	18-09-2014
		KR 20140053126 A	07-05-2014
		US 2014182681 A1	03-07-2014
		WO 2012175219 A1	27-12-2012
EP 2942826 A2	11-11-2015	EP 2942826 A2	11-11-2015
		EP 3185323 A1	28-06-2017